NUREG/CR-0312

EFFECT OF SCALE ON TWO-PHASE COUNTERCURRENT FLOW FLOODING

Final Report
July 1977 - June 1978

H. J. Richter
G. B. Wallis M. S. Speers

Thayer School of Engineering
Dartmouth College

Prepared for
U. S. Nuclear Regulatory Commission

Available from
National Technical Information Service
Springfield, Virginia 22161

NUREG/CR-0312
R2

EFFECT OF SCALE ON TWO-PHASE COUNTERCURRENT FLOW FLOODING

Final Report
July 1977 - June 1978

H. J. Richter
G. B. Wallis M. S. Speers

Thayer School of Engineering
Dartmouth College
Hanover, PA 03755

Manuscript Completed: July 1978
Date Published: June 1979

Prepared for
Office of Nuclear Regulatory Research
U. S. Nuclear Regulatory Commission
Washington, D.C. 20555
NRC FIN No. B5816

ABSTRACT

Air-water countercurrent flow experiments have been performed in vertical tubes of different sizes and in annuli with different gap sizes. The gas velocity sufficient to produce zero penetration of liquid in large tubes (6" and more) and annuli seems to be the same.

For 2" diameter tubes the flooding behavior can be represented by the Wallis correlation.

In large tubes and annuli it was assumed that all liquid penetrated in the form of a film along the walls. A force balance on this liquid film leads to a correlation, which predicts the flooding behavior in most cases satisfactorily.

TABLE OF CONTENTS

LIST OF FIGURES

ACKNOWLEDGMENT

This work was sponsored by the Nuclear Regulatory Commission (NRC) under Contract No. NRC-04-76-329.

ABBREVIATIONS AND SYMBOLS

A	flow cross section
b	width
C	constant in Wallis correlation eq.(1)
$(C_f)_i$	interfacial friction factor
C'	constant eq.(12)
C_w	wall friction factor
D	tube diameter, hydraulic diameter
D^*	dimensionless diameter eq.(5)
g	gravity constant
h	height
j_f	liquid flux
j_f^*	dimensionless liquid flux
j_g^*	dimensionless gas flux
j_i	dimensionless liquid or gas flux eq.(2)
J_i^*	dimensionless liquid or gas flux eq. (3)
Ku	Kutateladze number eq.(4)
N_B	Bond number eq.(14)
Δp^*	Nondimensional pressure drop $\Delta p^* = \frac{\Delta p}{(\rho_f g D)}$
Q_i	liquid or gas volumetric flux
v_f	liquid velocity
v_g	gas velocity
v_i	interfacial velocity
w	circumference
δ	gap size
δ_f	film thickness
δ_f'	amplitude of wave
μ	weir coefficient
ρ_f	liquid density
ρ_g	gas density
ρ_i	liquid or gas density
σ	surface tension
τ_i	interfacial shear stress
τ_w	wall shear stress

EFFECT OF SCALE ON TWO-PHASE COUNTERCURRENT FLOW FLOODING

1. INTRODUCTION

The simultaneous flow of liquid down and gas up in a vertical conduit has its limitations. The higher the gas flow rate up, the lower is the water flow rate which can penetrate down. This limit of countercurrent flow is called "flooding". It is of major importance in connection with Nuclear Reactor Safety and the operation of Emergency Core Cooling Systems.

Past experiments have resulted in a number of correlations to predict the flooding behavior. Of special interest are the Wallis correlation, which describes the whole flooding curve, and the work of Pushkina and Sorokin, who measured the gas velocity necessary to prevent liquid penetration downwards. The Wallis correlation has worked very well in small tubes. Pushkina and Sorokin performed a rather thorough study with air and water in various diameters to determine the zero water penetration point. Unfortunately, there is substantial disagreement between the Wallis correlation and Pushkina and Sorokin's work when the tube is 6 inches or more in diameter.

In addition, it is questionable whether the above mentioned correlations can be used to describe flooding in reactor-like geometries such as an annulus. The goals of this work were:

1) to determine which correlation, if any, describes zero penetration (i.e. duplicate or fail to duplicate Pushkina and Sorokin's work) in different size tubes and annuli;

2)to measure substantial portions of the flooding curve in different size tubes and annuli;

3) to derive an analytical model based on the observations in the experiment.

2. TECHNICAL BACKGROUND

As a result of experimental studies of countercurrent flow several dimensional groups have emerged because they correlate flooding data quite well. One equation in use correlates the liquid flux vs. the gas flux at the flooding limit (Wallis' correlation)

$$j_g^{*\frac{1}{2}} + j_f^{*\frac{1}{2}} = C \qquad (1)$$

where j_g^* and j_f^* are the dimensionless fluxes of the gas and liquid

$$j_i^* = \frac{\rho_i^{\frac{1}{2}} j_i}{\{g D(\rho_f - \rho_g)\}^{\frac{1}{2}}} \qquad (2)$$

with D the diameter of the tube or the hydraulic diameter of an annulus.

Some investigators claim that the circumference is more appropriate as the characteristic length than the hydraulic diameter for an annulus and define a flux

$$J_i^* = \frac{\rho_i^{1/2} \; j_i}{\{g \; w(\rho_f - \rho_g)\}^{1/2}} \tag{3}$$

where $w = \pi D$ is the average circumference of an annulus. In both equations $j_i = \frac{Q_i}{A}$ represents the velocity of gas or liquid if it would flow alone in the cross section.

The other correlation deals with the extreme case of flooding, the zero penetration of liquid flow down. This theory claims that surface tension is important in determining the limit to countercurrent flow, leading to the so-called Kutateladze number:

$$Ku = \frac{\rho_g^{1/2} \; j_g}{\{g \; \sigma(\rho_f - \rho_g)\}^{1/2}} \tag{4}$$

The ratio of Eq.(1) and (4) gives a dimensionless diameter.

$$D^* = D\left[\frac{g(\rho_f - \rho_g)}{\sigma}\right]^{1/2} \tag{5}$$

From Eq.(1) we predict for zero penetration ($j_f^* = 0$) the solution $j_g^* = C^2$ or $j_g \propto D^{1/2}$ for constant thermodynamic properties. From Eq.(4) the zero penetration point is at j_g = const. for the same conditions. Thus an obvious contradiction between the two correlations occurs. While Eq.(1) would predict a larger and larger gas velocity with increasing pipe size, the second correlation claims that the gas velocity for zero penetration is virtually independent of pipe size.

One could argue that in large tubes the criterion for zero penetration of liquid should be at Ku = const. if the liquid is in the form of a film much thinner than the tube diameter, so that surface tension is important for determining the "characteristic dimension". In smaller tubes, where the tube diameter is the "characteristic dimension", the right criterion for zero penetration might be sought in j_g^* = const. or $j_g \propto D^{1/2}$.

A methodical approach to the influence of different scales on flooding phenomena has been started under this program. Tubes of different diameter were tested with symmetrical "top flood" (i.e. the water is sup-

plied at the top of the tube rather than somewhere along the length) to measure the onset of downwards water flow while air was flowing upwards in the pipe. Results have been presented by Richter and Lovell (1977). Since then the experiments were continued to include nonsymmetrical water injection into the tube to study the influence on the flooding behavior and a new test facility was built to provide experimental results for annuli with two different gap sizes with symmetrical as well as nonsymmetrical top flood.

3. EXPERIMENTAL FACILITIES

The first test facility for studying flooding in tubes of different sizes is shown in Figure 1. It consists of a vertical transparent pipe about 40 inches long and an upper and lower plenum. A 55 gallon drum was used to construct the upper plenum. Water enters through a 2 inch pipe into the upper plenum at rates up to about 250 gpm.

An overflow was cut out of the side of the upper plenum and excess water is drained away via spillway.

An aluminum bottom has been specially constructed and fitted to the bottom of the upper plenum. Using a neoprene gasket, the plexiglass "flooding tube" can be adjusted to protrude into the upper plenum as desired.

The "flooding tube" is vertical and with square cut ends, unpolished. Experiments were performed in 2", 6" and 10" diameter pipes; all were 40-48 inches long.

The lower plenum is also constructed from a 55 gallon drum. Air enters the side of the lower plenum via a 10 inch pipe. Water reaching the lower plenum (water "penetration") is allowed to collect, and thus the penetration volumetric water flow rate Q_f is measured.

Both upper and lower plena have plexiglass windows to allow observation of entrance/exit conditions of the flooding tube. The lower plenum can be drained by means of a tight closing butterfly valve in the drainage pipe. Air flow into the lower plenum is controlled by butterfly valves and measured by an orifice plate and pressure taps leading to a manometer.

The air supply is a 75 H.P. blower with a maximum flow rate of 2100 scfm at a maximum pressure rise of 5 psig.

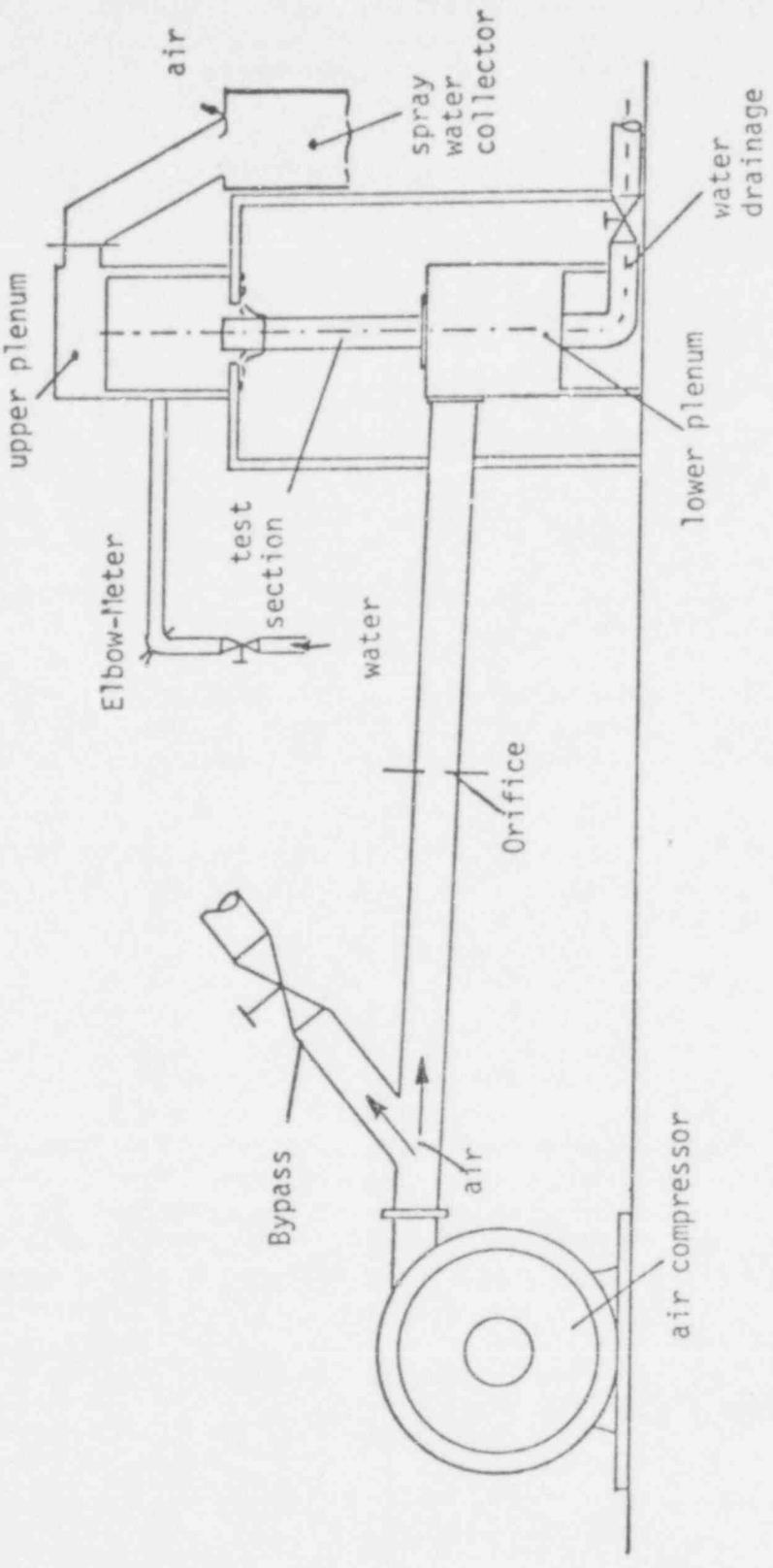

Figure 1 Experimental set up for flooding in large tubes

This test facility was later modified to allow nonsymmetrical top flood experiments, see Figures 2 and 3. For the first tests of non-symmetrical water inflow into the flooding tube a skirt extending 3 inches above the upper end of the test section was wrapped around 270° (3/4) of the circumference of the test pipe. This provided water flow into the test section only from 1/4 of the circumference as long as the liquid head in the upper plenum above the tube was smaller than the skirt height of 3 inches.

For the second series of tests the water was inserted directly down into the flooding tube through either a 2 inch or 1 inch exit diameter nozzle, see Figure 3.

The second test facility was built around an annulus test section, see Figure 4. The plexiglass tube for the annulus has an inside diameter of 17.5" and is approximately 40" long. Two interchangeable inner tubes (core) have 15.5" and 13.5" outside diameters thus providing annulus gap sizes of 1" or 2". The upper and lower plena are 40" diameter barrels with plexiglass windows. The water that penetrated into the lower plenum was collected there.

For the air supply and the measurement of the air flow the same facility was used as for the tube experiments. The annulus test facility was modified to allow nonsymmetrical top flood as well. As in the tube experiments a flow skirt was wrapped around 270° (3/4) of the annulus. It extended about 9 inches above the top of the outside flooding tube, see Figure 5. This provided water flow into the annulus only from 1/4 of the circumference, thus encouraging a nonsymmetrical behavior.

4. EXPERIMENTAL RESULTS

TUBE EXPERIMENTS

The experimental results of the symmetrical top flood experiments in tubes were presented by Richter and Lovell (1977). It was found that for zero penetration in large tubes a Kutateladze number of approximately 3.2 seems to be appropriate. The flooding curve, plotted on j* coordinates was found to be dependent on the size of the pipe. Experimental results with a 2" diameter tube resembled the Wallis correlation very well, while the flooding curve shifted with increasing pipe size to smaller values of the dimensionless fluxes j_f^* and j_g^*, (see Figure 6).

The nonsymmetrical top flood experiments were performed in the 10" diameter tube. The results with the flow skirt around the top of the test section show essentially the same flooding behavior as was observed with the symmetrical top flood in the 10" diameter tube (see Figure 7). At low gas flow rates the liquid flow rate down is not limited by flooding but rather by the flow restriction due to the flow of water over the top end of the pipe, which can be compared to the flow over a weir. The theoretical points on the curve when the liquid volume flow rate is equal to the gas volume flow rate ($Q_g = Q_f$) were obtained by cal-

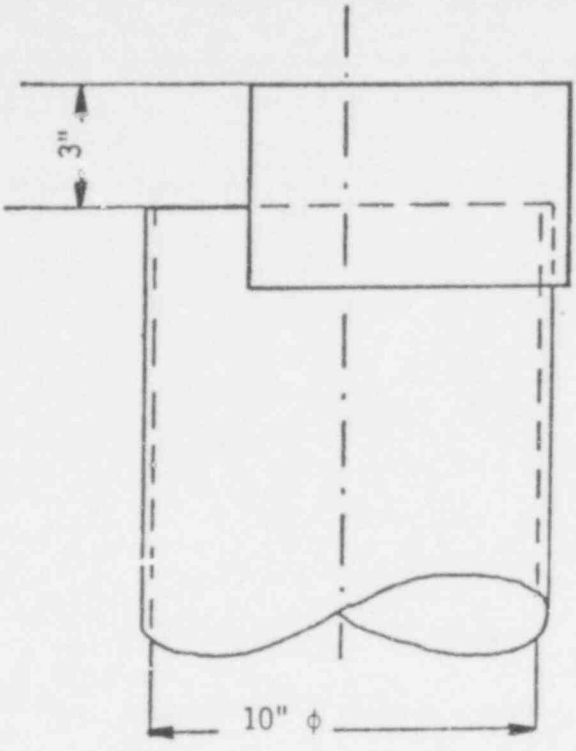

Figure 2. Nonsymmetrical flow skirt around the upper end of the pipe

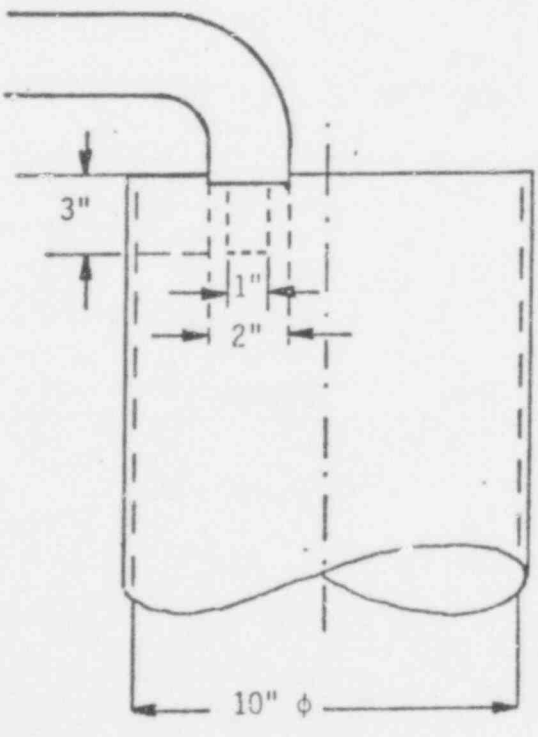

Figure 3. Water injection through 1 and 2 inch diameter nozzles

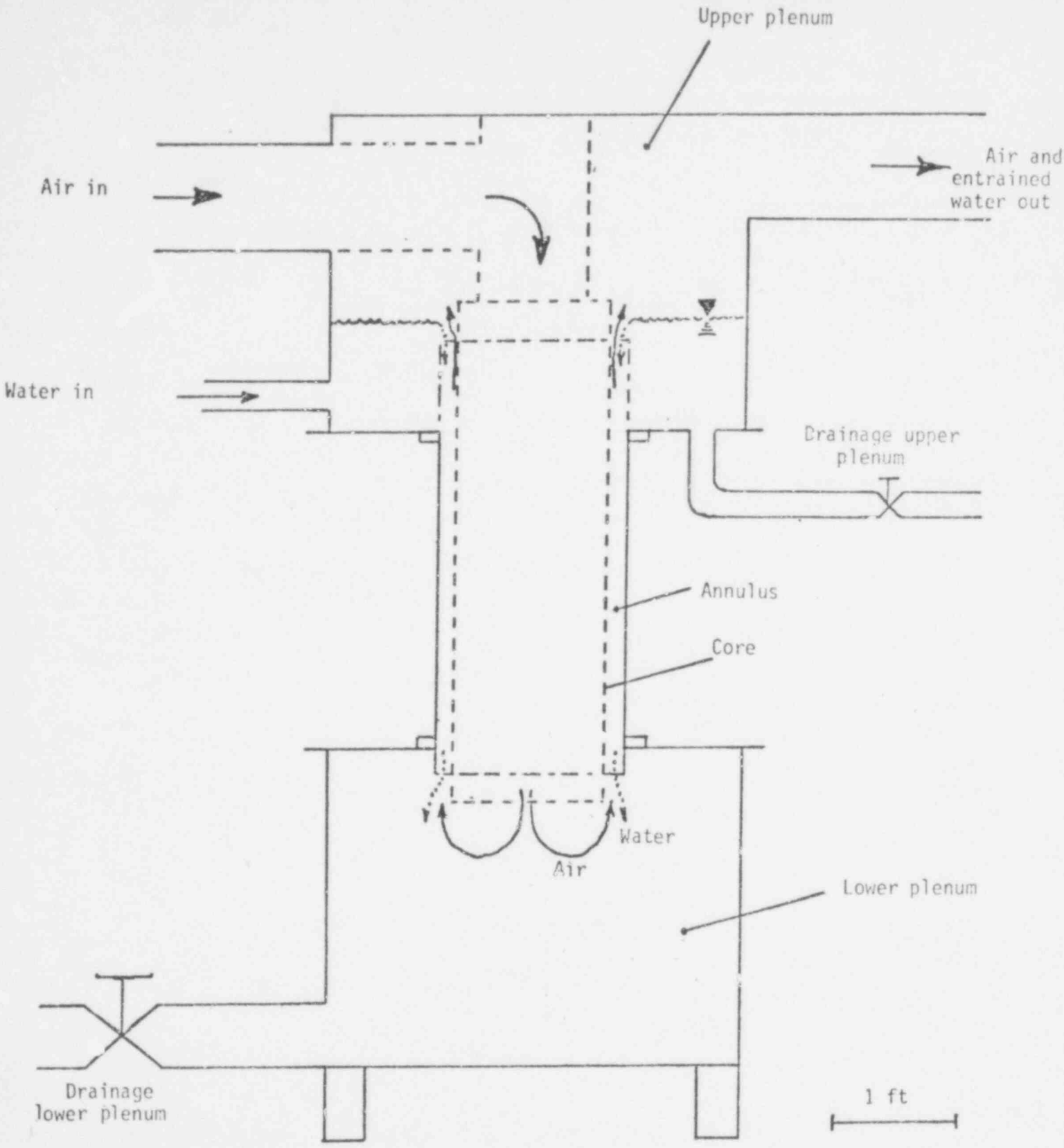

Figure 4. Annulus test facility

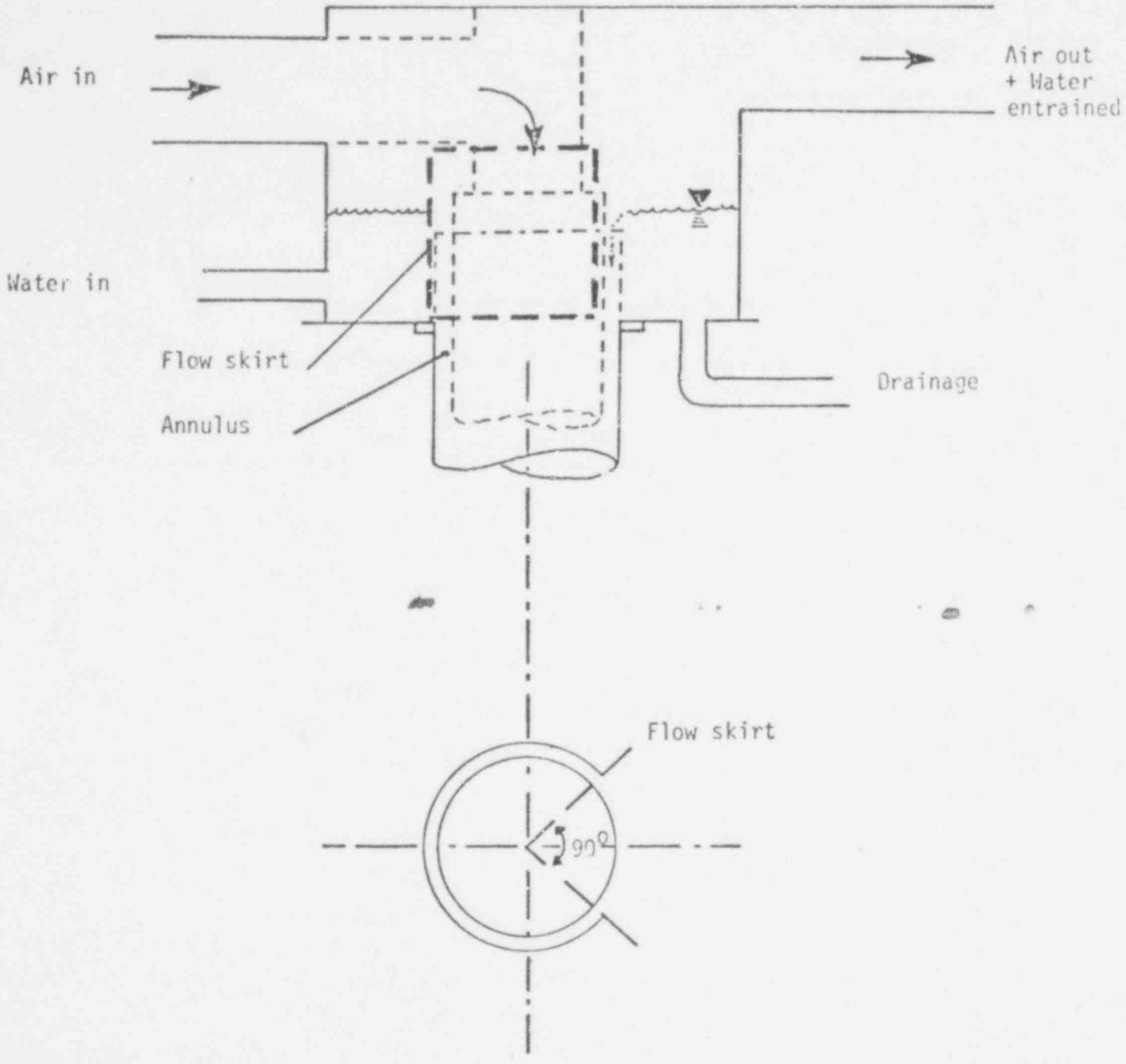

Figure 5 Flow skirt for nonsymmetrical water flow into annulus

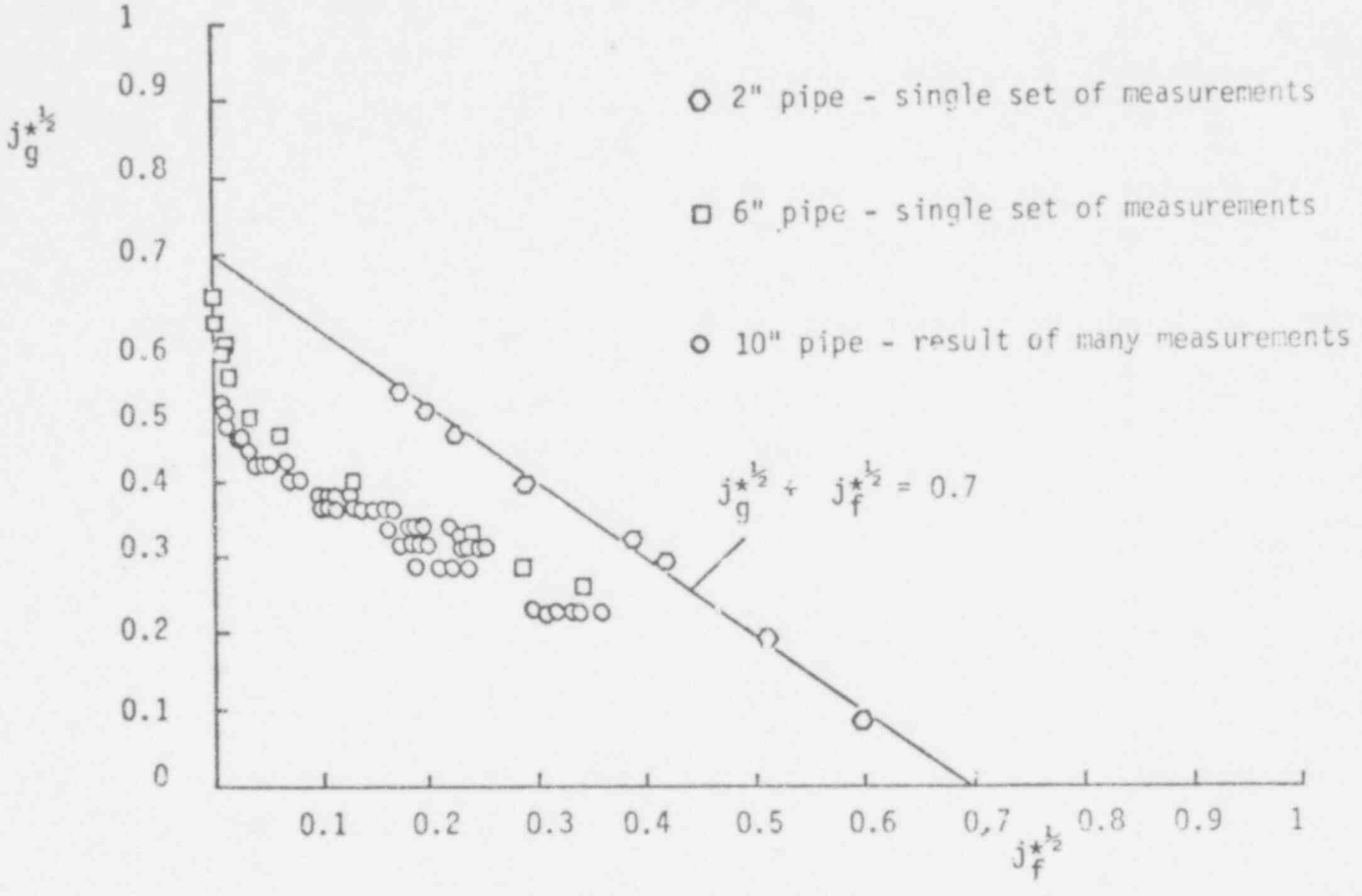

Figure 6. Nondimensional gas flux vs. water flux in different size pipe experiments

491 101

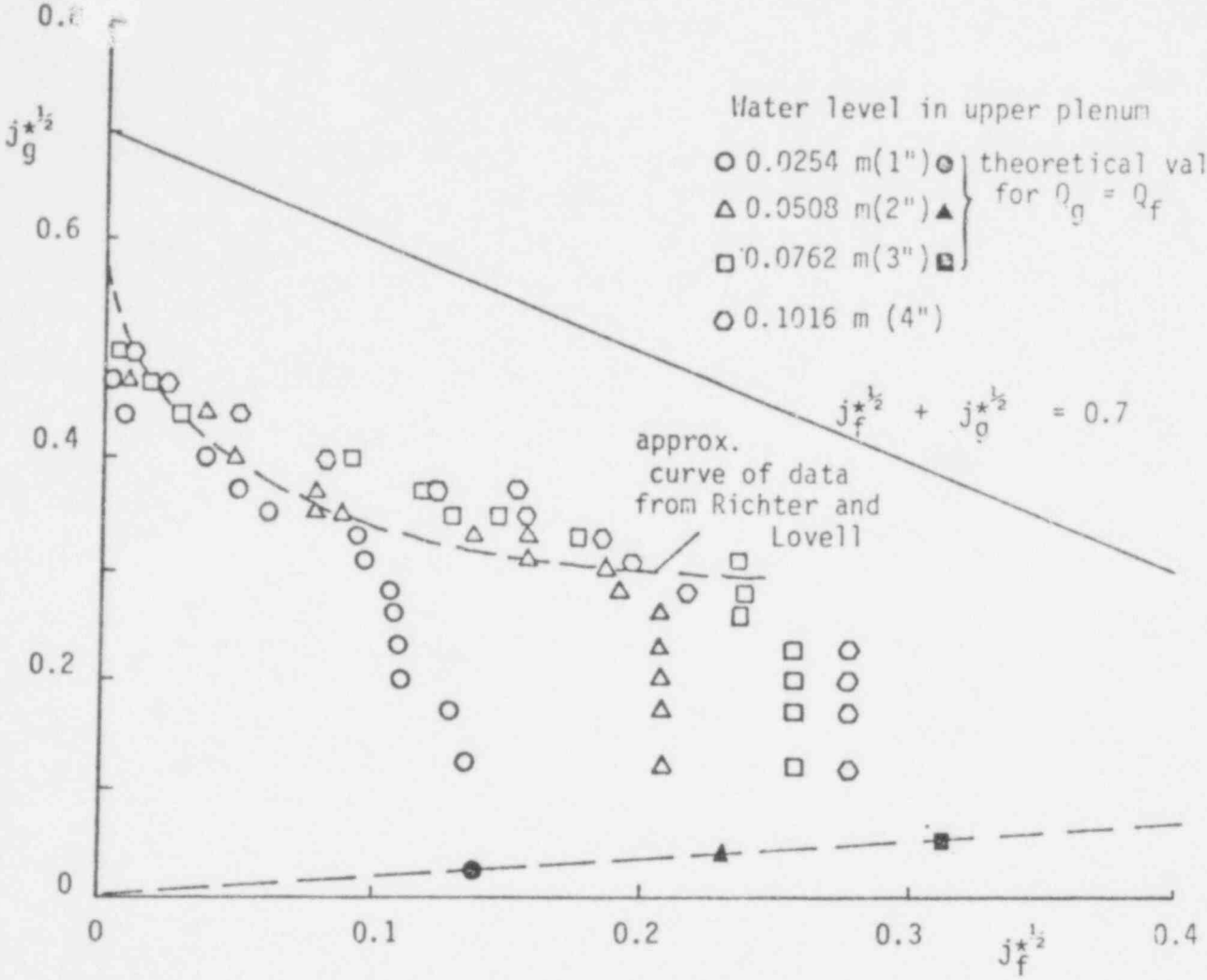

Figure 7. Flooding in 10 inch diameter tube with nonsymmetrical water flow from top, with several water levels in the upper plenum

culations of flow over a weir (see Appendix B). At low gas flow rates the deviation from the theoretical maximum water flow becomes more pronounced at higher water levels in the upper plenum. This is probably due to the restriction of the flow from the walls of the flow skirt. It was observed that the flow over the weir converged more at higher water levels. The theoretical point for a water level of 4" was not plotted since there was also water flowing over the top of the flow skirt into the flooding tube (flow skirt height was 3").

The following experiments were performed with a water jet pointing down into the flooding tube. The nozzle was inserted off center of the flooding tube (see Figure 3) in order to create a highly nonsymmetrical flow in the tube. It was speculated that the momentum of the jet would increase the water penetration. As can be seen from Figure 8 the penetration is enhanced compared to the data from Richter and Lovell. The maximum water velocity exiting from the nozzle was approximately 4 m/s (for 125 gpm) for the 2 inch diameter nozzle. A substantial increase in penetration was achieved for the same liquid flow rates through a 1 inch diameter nozzle,(see Figure 9). This smaller nozzle resulted in a water momentum sixteen times as large as for the 2 inch diameter nozzle at the same flow rate, increasing the penetration rate for some cases above the Wallis correlation. The limits of water penetration at low gas flow rates are equal to the water injection rate, where $j^*_{f\ in} = j^*_{f\ down}$ because no water is being expelled into the upper plenum.

Positioning of the nozzle exactly in the center of the flooding tube (only the 1" nozzle was used) increased the penetration rate of water slightly,(compare Figures 9 and 10). This is probably due to the fact that less water of the jet impinges on the wall of the tube in this case. As soon as water impinges on the wall, a film is formed which travels upwards at the high gas velocities.

ANNULUS EXPERIMENTS

The experiments in the annulus test facility were performed to obtain data on zero penetration as well as to measure the flooding curve. Since it was found in the tube experiments that the flooding behavior depended upon the water level in the upper plenum as long as the water level was lower than 4", this water level was one variable in these experiments. Quite extensive measurements have been done to verify the zero penetration point, which was found to be in the range of a Kutateladze number of 3.4 for the 1" gap and about 3.0 for the 2" gap. The zero penetration was found not to be a function of the water level in the upper plenum. Yet the flooding tests showed a strong dependency of water level on flooding behavior for water levels smaller than 4" (see Figure 11 for experimental results of the 1" annulus gap). As a reference line the Wallis correlation is plotted with a constant of C = 0.7 (all data points of the annulus experiments are listed in Appendix A). The points on the $Q_g = Q_f$ line are measured water pene-

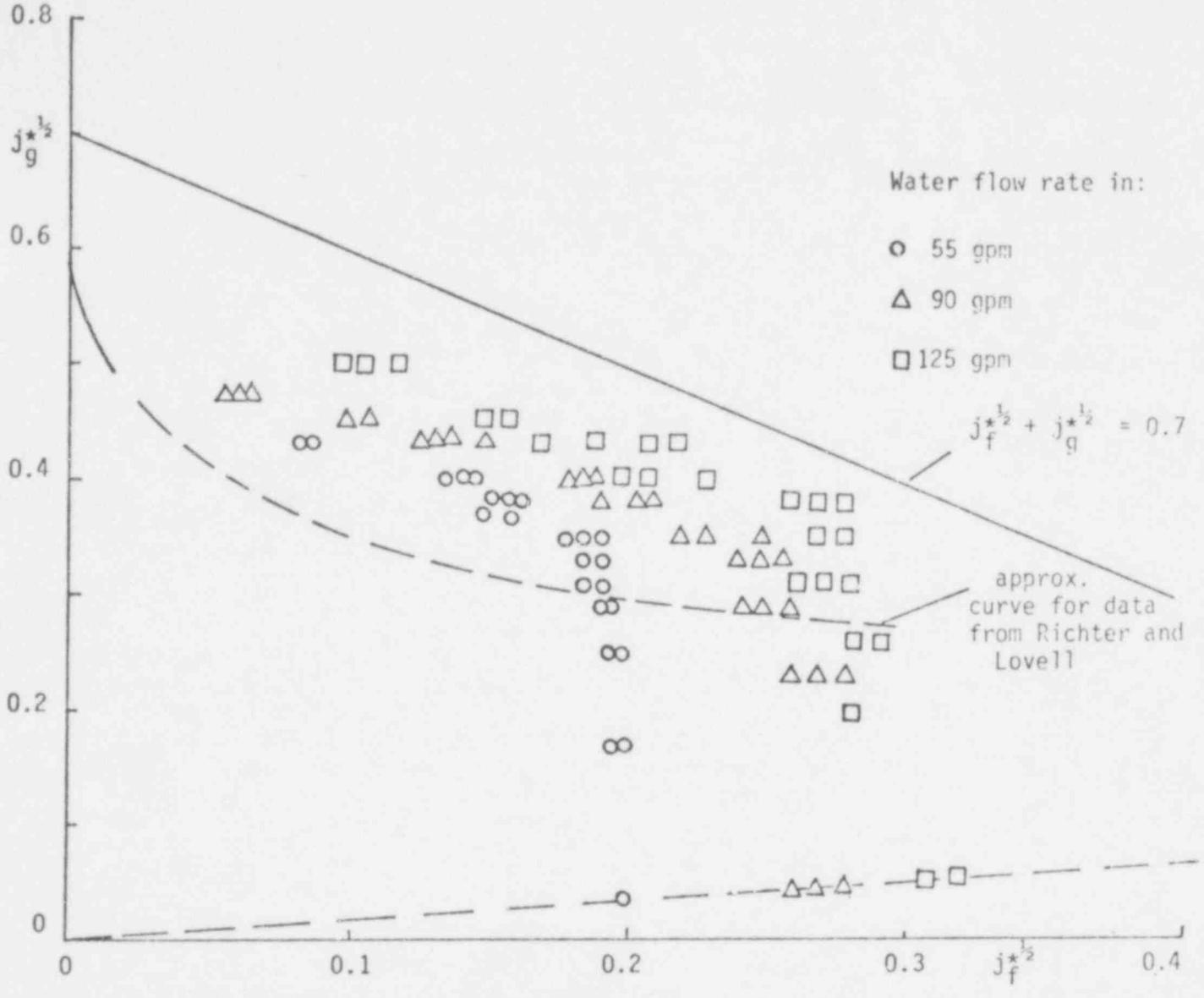

Figure 8. Flooding in 10 inch diameter pipe with a water jet down through a 2 inch diameter nozzle.

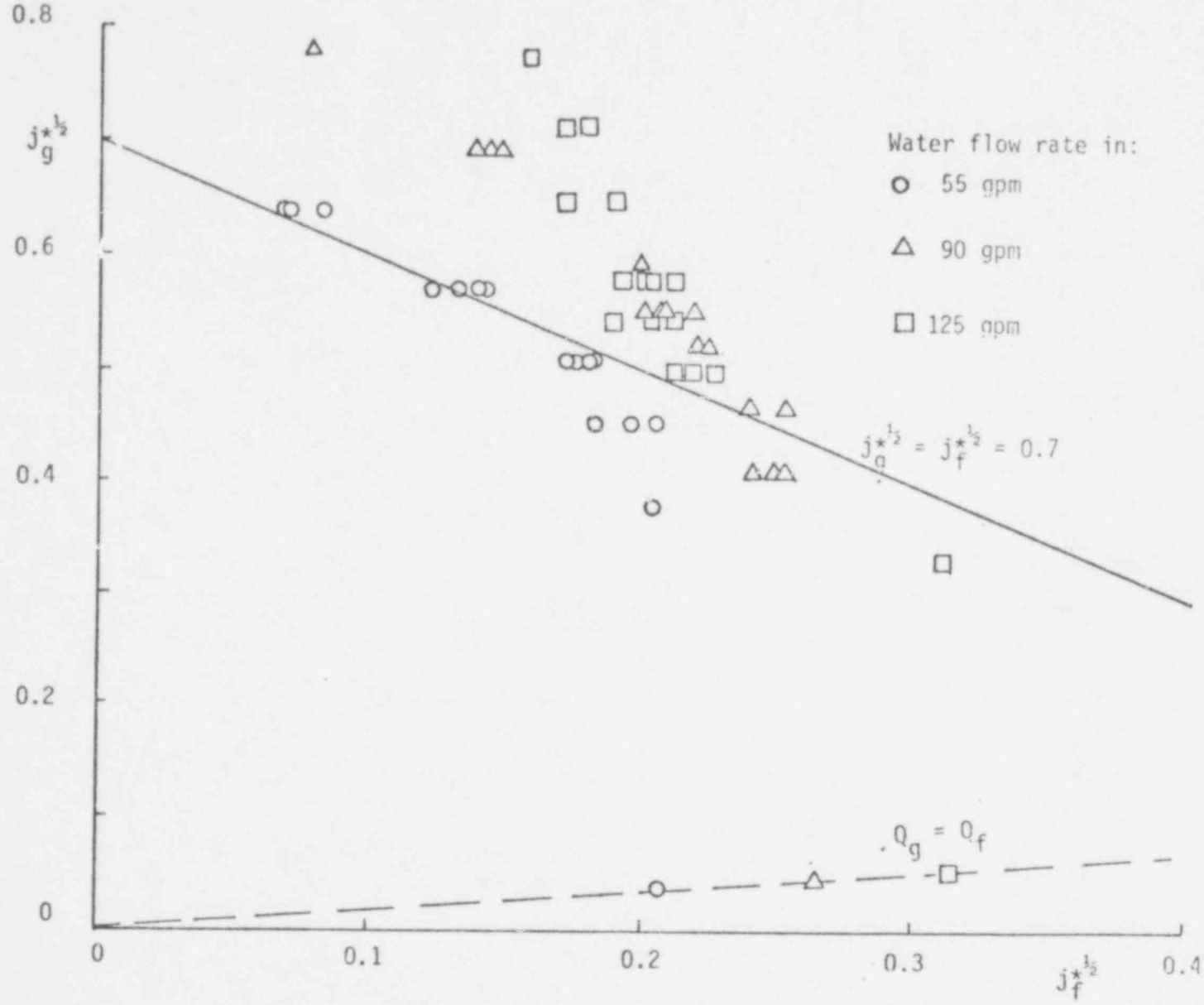

Figure 9. Flooding in 10 inch diameter tube with a water jet down through a 1 inch diameter nozzle

491 105

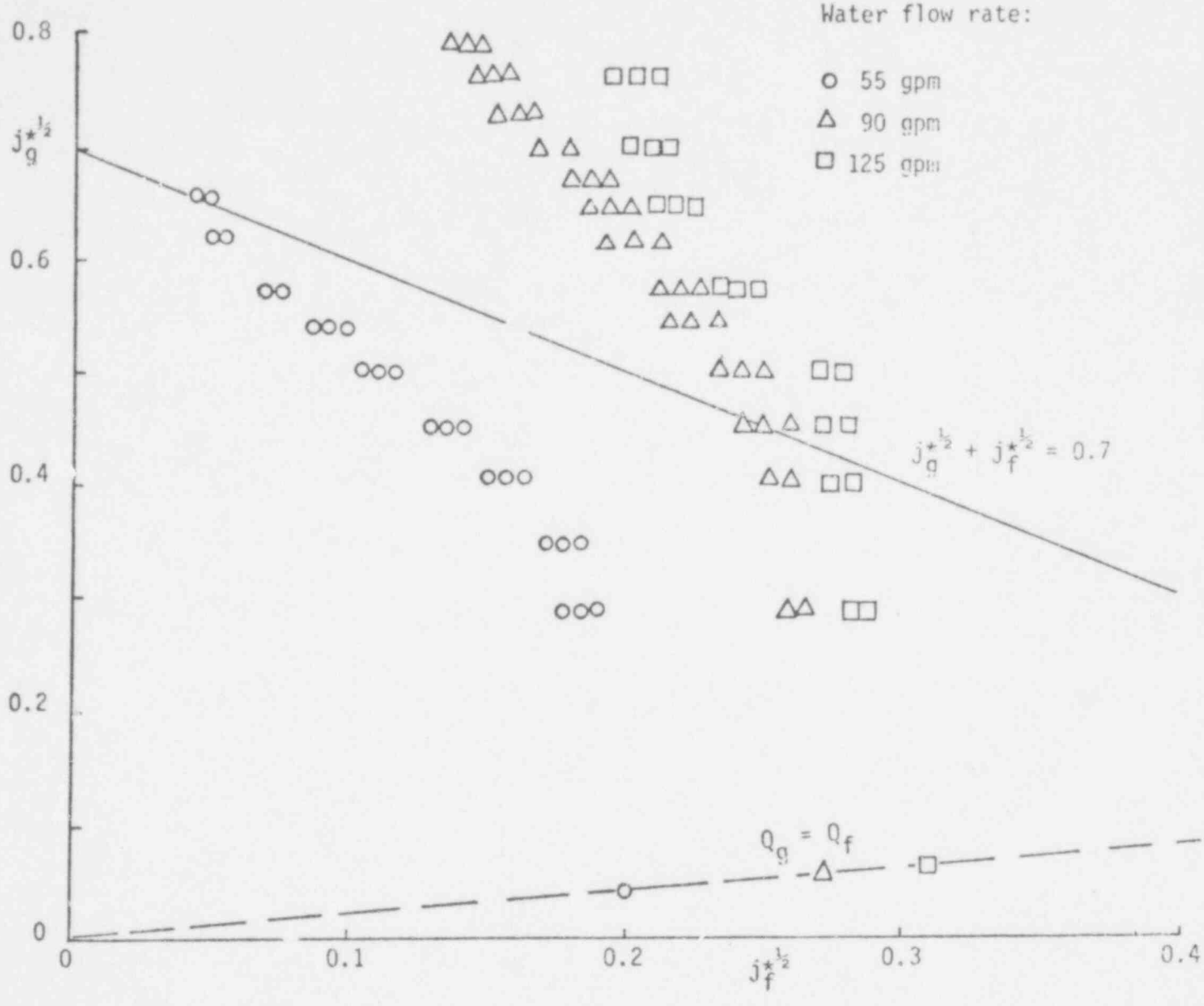

Figure 10. Flooding in a 1½ inch diameter tube with a water jet down through a 1 inch diameter nozzle in the center of tube

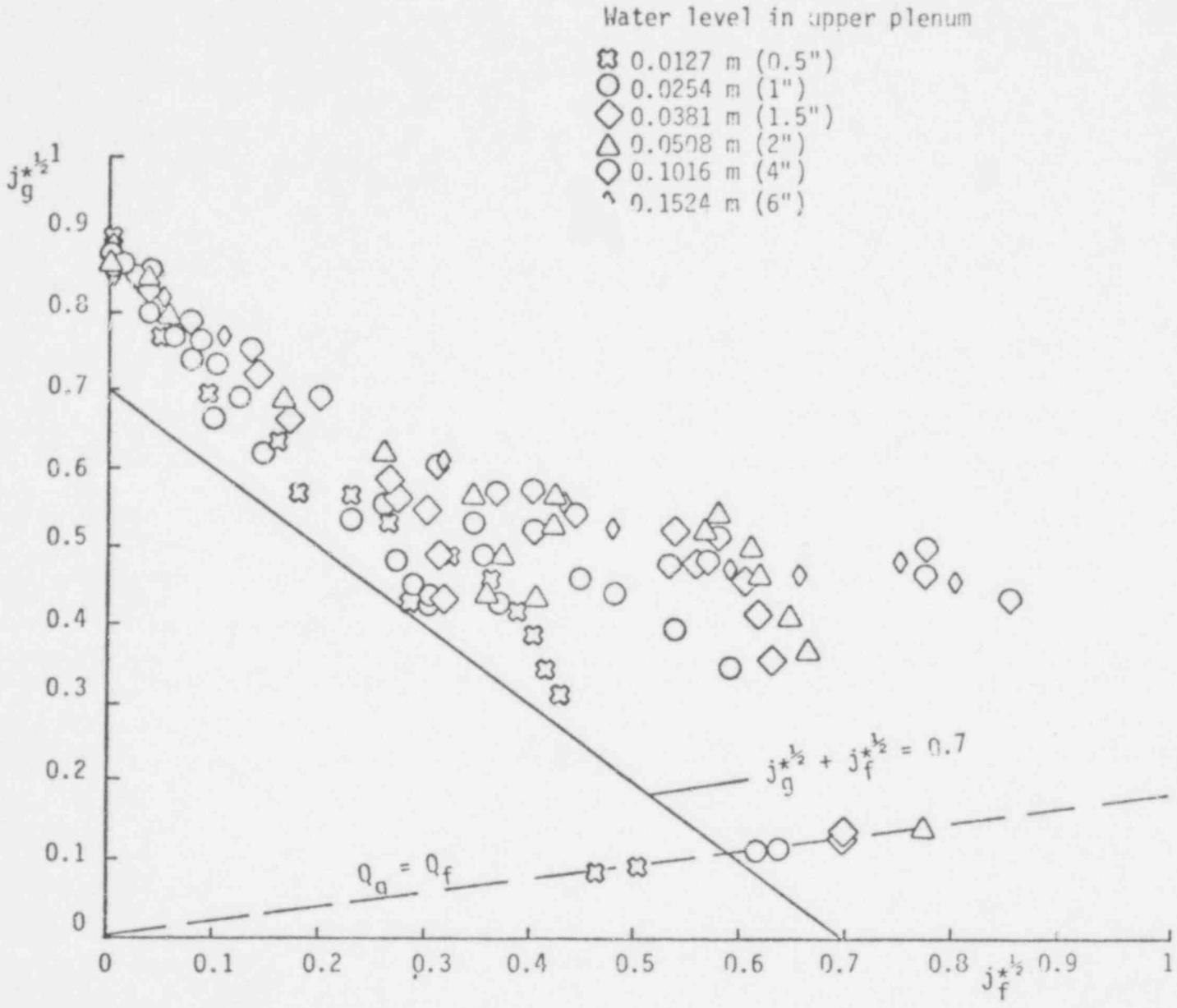

Figure 11 Nondimensional gas flux vs water flux in the 1 inch annulus gap with different liquid levels in upper plenum. Symmetrical top flood.

tration rates when the blower is not running. The gas volume in the lower plenum is displaced by the penetrating water volume, thus $Q_g = Q_f$. There is a large difference in water penetrating for the different water heights in the upper plenum. For the same gas flow rate (j_g^* = const.) the water penetration rate increases with increasing water level, up to water heights of 2" to 4" above which there is no difference in flooding behavior. In the tube experiments, where similar observations were made, this was attributed to liquid "bridging" in the upper plenum causing the gas to bubble through the water.

Figure 12 shows the flooding behavior for the annulus experiments with a 2" gap. The results show clearly two distinctly different classes of results, a lower penetration rate for water levels up to 2" in the upper plenum and one for water levels of 4" and above. The drop off of the high water level data (4"and 6") at high water penetration rates is probably due to the fact that these rates are close to the maximum water flow which can be provided.

As mentioned before, experiments were performed in the annulus test facility with a nonsymmetrical top flood as well. A flow skirt was wrapped 270° (3/4) around the top of the annulus extending 9" above the top of the annulus. In Figure 13 the symmetrical top flood data are compared with the nonsymmetrical flow results for water levels of 1" and in Figure 14 for 4" above the annulus in the upper plenum for a 1" annulus gap. Penetration rate is enhanced for the nonsymmetrical top flood, e.g. for a water level of 4" and a gas flux of $j_g^{*\frac{1}{2}} \approx 0.55$ the water penetration rate is $j_f^{*\frac{1}{2}} = 0.6$ instead of $j_f^{*\frac{1}{2}} = 0.4$ for the symmetrical top flood, which means an increase in penetration rate of more than a factor of two. Zero penetration occurs at the same gas flux independent of whether the water is supplied symmetrically or nonsymmetrically.

For a 2" annulus gap with nonsymmetrical top flood we see a very similar trend. The penetration rate increases for the nonsymmetrical top flood (see Figures 15 and 16).

5. ANALYSIS

The analysis used by Richter and Lovell to predict the flooding behavior in tubes can also be used for flooding in the annulus. This theory assumes that initial penetration occurs in the form of a thin annular film. This film is balanced against gravity by wall shear τ_w and interfacial shear forces τ_i . Thus a force balance can be set up between the weight of a film and the shear forces:

$$\tau_w + \tau_i = \delta_f(\rho_f - \rho_g)\, g \qquad (6)$$

where δ_f is the average film thickness.

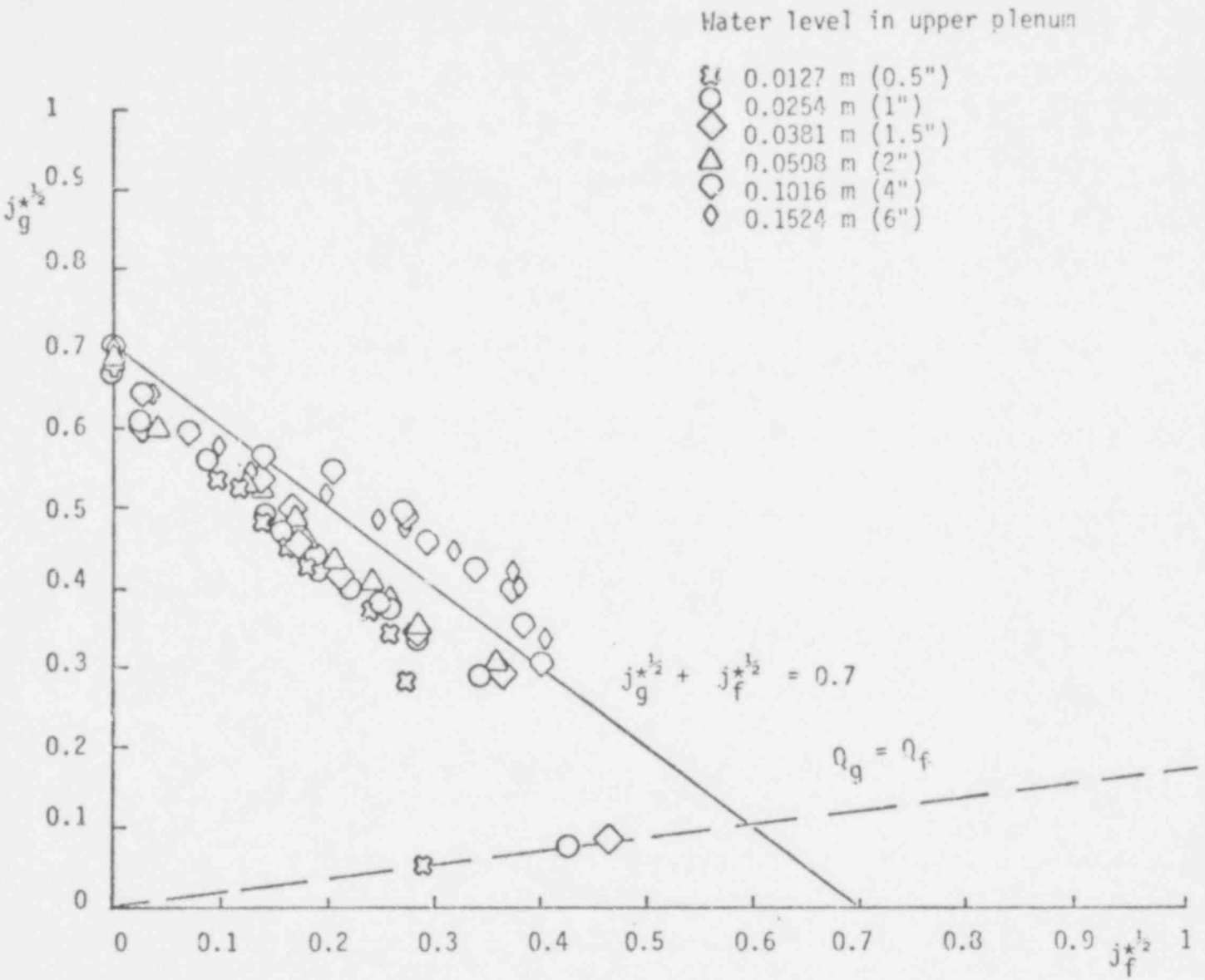

Figure 12 Nondimensional gas flux vs. water flux in the 2 inch annulus gap with different liquid levels in upper plenum. Symmetrical top flood.

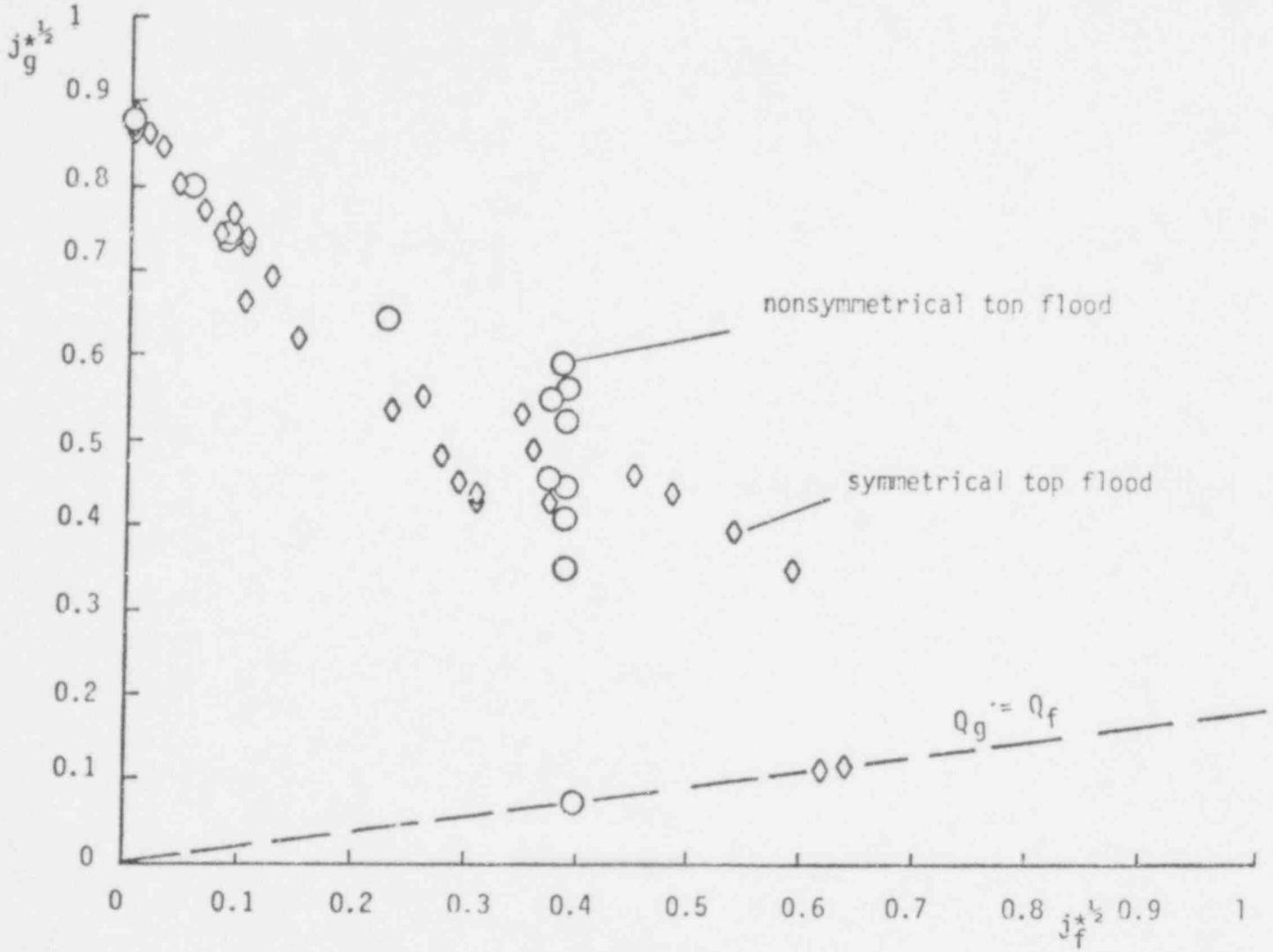

Figure 13 Nondimensional gas flux vs water flux in the 1 inch annulus gap. Comparison of symmetrical and nonsymmetrical top flood data for 0.0254 m (1") water level in upper plenum.

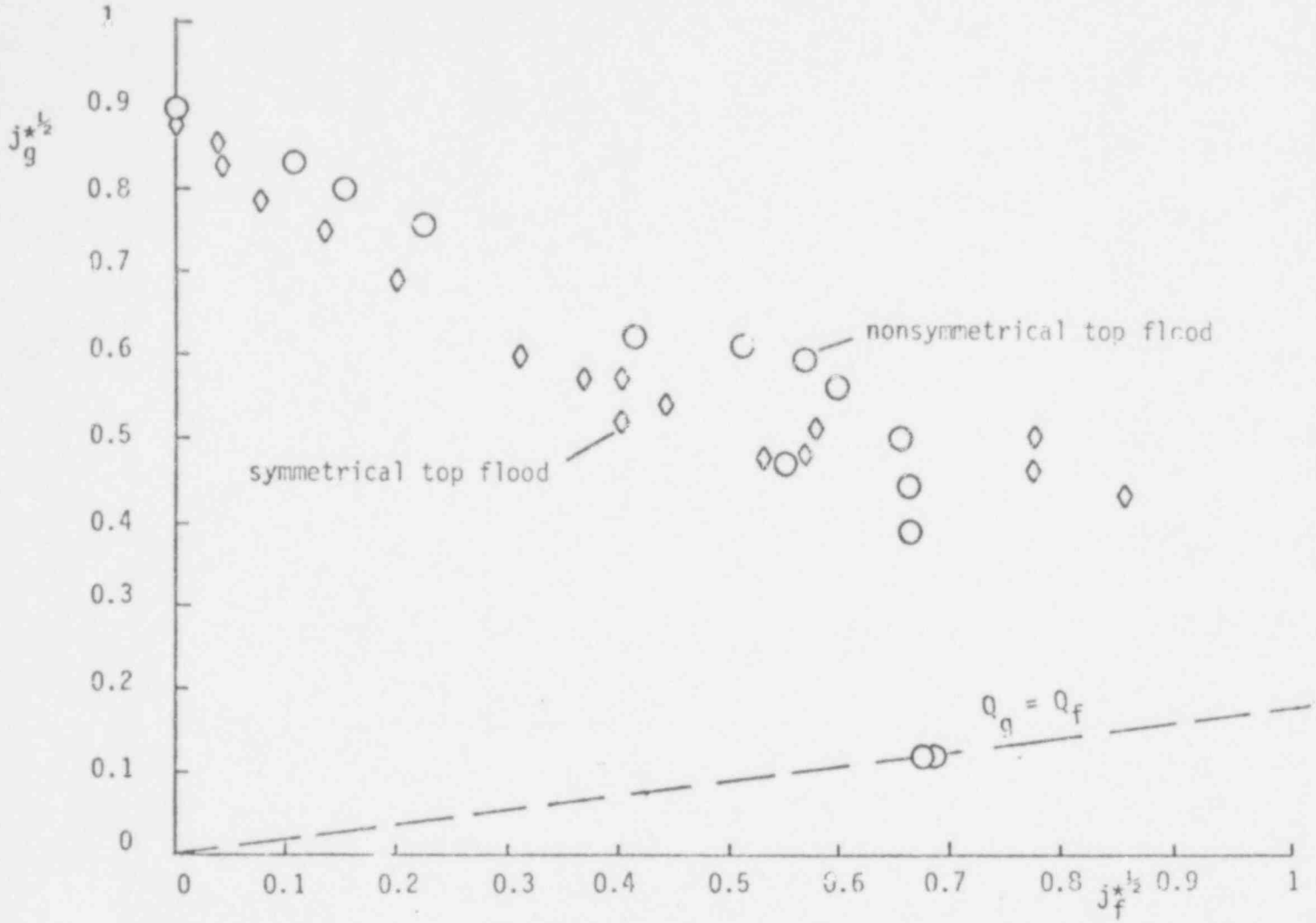

Figure 14. Nondimensional gas flux vs. water flux in the 1 inch annulus gap. Comparison of symmetrical and nonsymmetrical top flood data for 0.1016 m (4") water level in upper plenum.

491 111

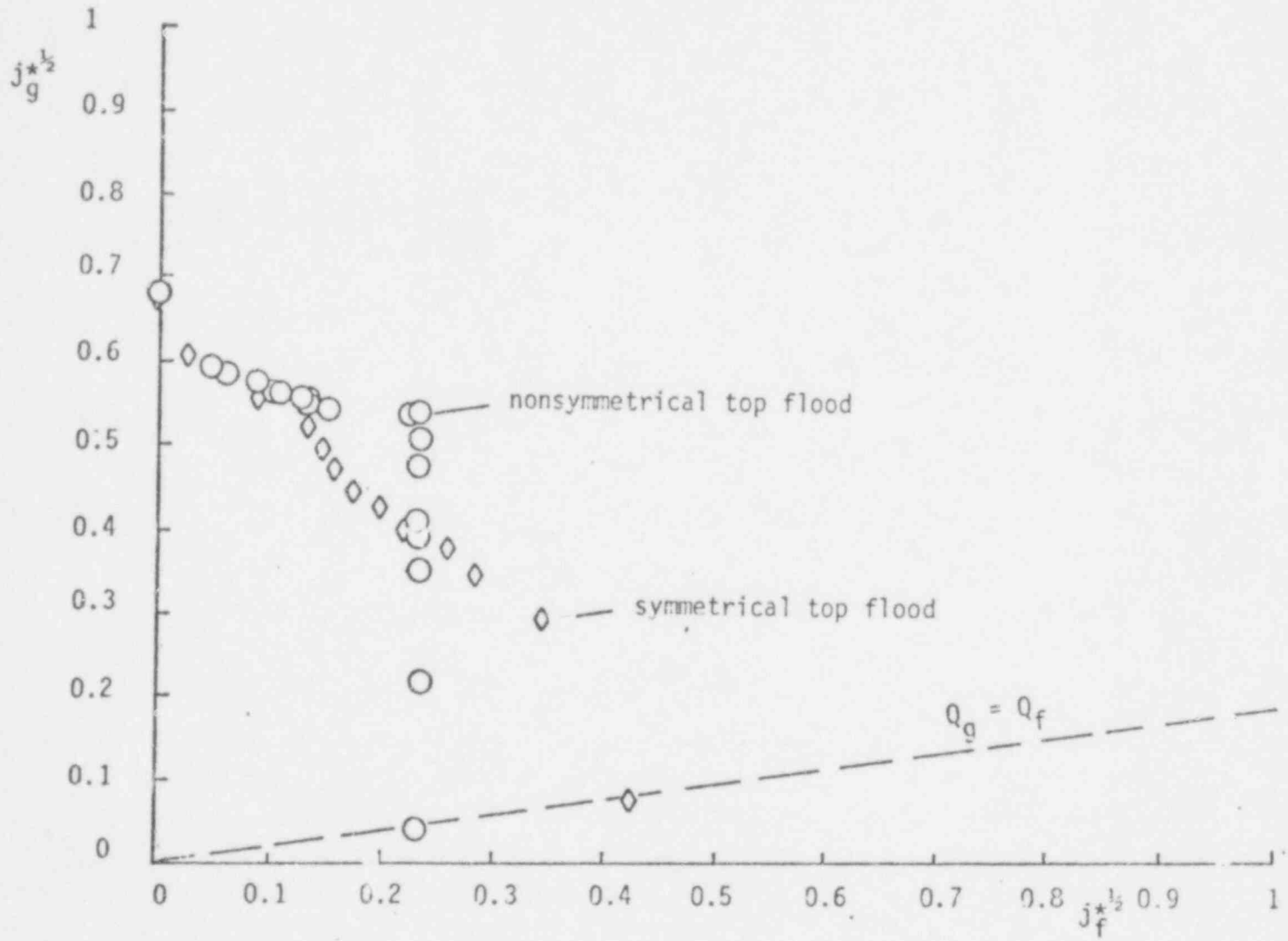

Figure 15 Nondimensional gas flux vs water flux in the 2 inch annulus gap. Comparison of symmetrical and nonsymmetrical top flood data for 0.0254 m (1") water level in upper plenum.

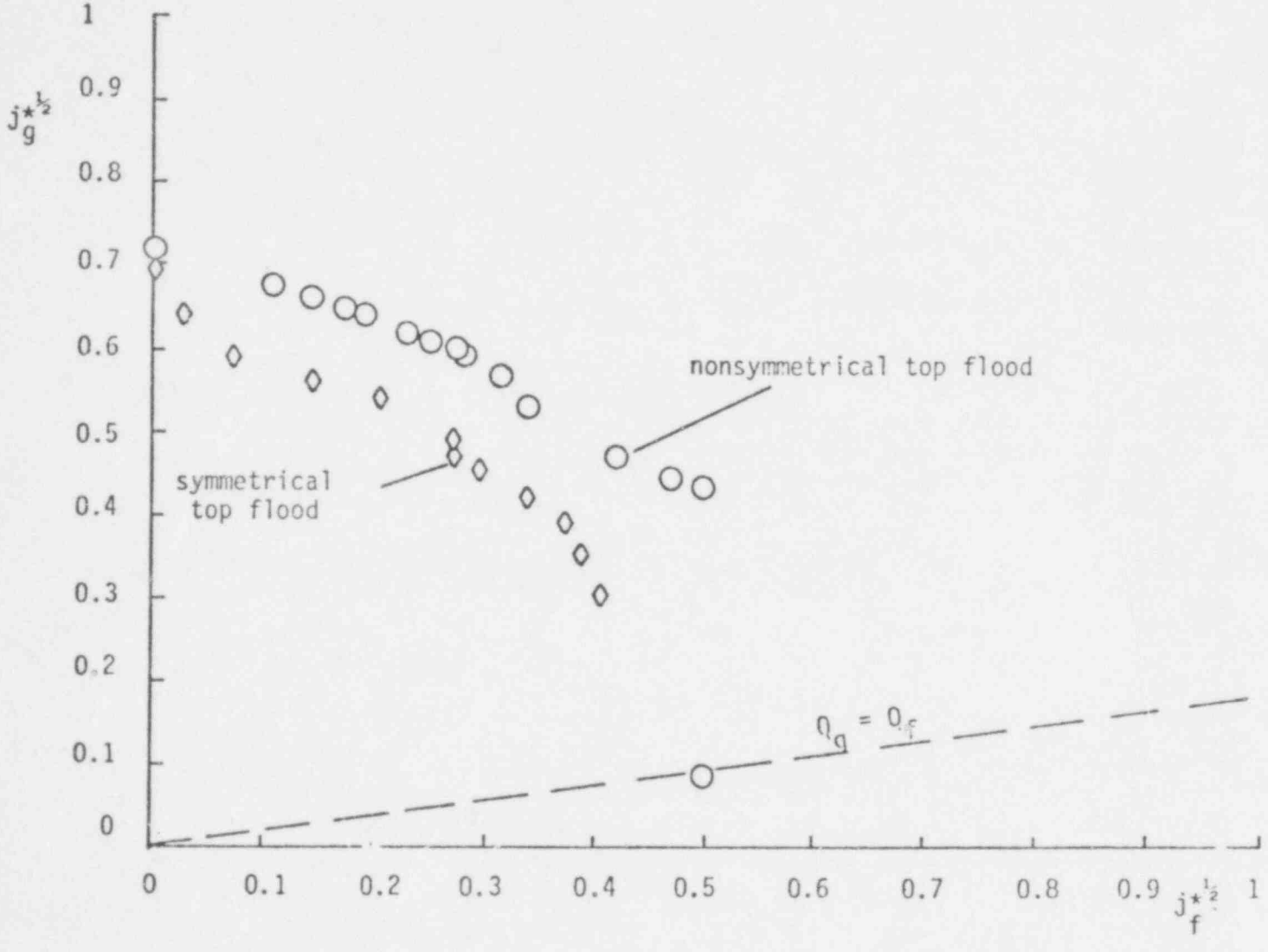

Figure 16 Nondimensional gas flux vs. water flux in the 2 inch annulus gap Comparison of symmetrical and nonsymmetrical top flood data for 0.1016 m (4") water level in upper plenum.

491 113

The wall shear stress can be expressed in terms of the average liquid velocity v_f

$$\tau_w = \frac{1}{2} C_w \rho_f v_f^2 \tag{7}$$

where C_w is a wall friction coefficient. We will set $C_w = 0.005$ in a smooth pipe. The interfacial shear force on this film is taken to be,

$$\tau_i = (C_f)_i \frac{1}{2} \rho_g (v_g + v_i)^2 \tag{8}$$

where v_g is the gas velocity and v_i is the liquid film surface velocity. Since the film is rather thin compared to the total cross section even in an annulus, we can introduce $v_g \approx j_g$ and

$$v_f = \frac{D}{4\delta_f} j_f \tag{9}$$

where D is the hydraulic diameter.

In the case of an annulus the hydraulic diameter D is twice the gap size, thus in equation (9) it is assumed that both walls of the annulus are wet and the film thickness on both walls is the same. As was observed this is not the case in all experiments. At low water levels in the upper plenum the outside wall seemed to carry most of the water flow, while on the inside wall a much thinner film was penetrating. Thus in the theoretical calculations it was assumed either that both walls were covered by an identical film or that the outside wall alone carried the entire flow. The interfacial film velocity v_i was assumed to be much less than the air velocity i.e. $v_i << j_g$ and therefore was neglected in this analysis. The interfacial friction coefficient could then be taken from cocurrent flow, see Wallis (1969).

$$(C_f)_i = 0.005 \left(1 + 300 \frac{\delta_f}{D}\right) \tag{10}$$

Introducing these assumptions, substituting Eqs. (7), (8), (9), and (10) into (6) will give a function relating j_f, j_g and the film thickness δ_f. The film thickness δ_f has to be estimated. If we assume a wave shaped as in the sketch we can write a force balance between the stagnation point in front of the wave and the top of the wave, the pressure

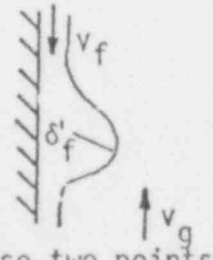

difference between these two points is approximately the dynamic head of the

gas if we neglect the wave velocity, thus we can write:

$$\frac{\sigma}{\delta_f'} \approx \frac{1}{2} \rho_g v_g^2$$

or

$$\delta_f' \approx \frac{2\sigma}{\rho_g v_g^2} \tag{11}$$

Wallis suggests that for cocurrent flow the roughness of the film $\delta_f' \approx 4\delta_f$. Introducing this we get for the film thickness

$$\delta_f \approx \frac{1}{2} \frac{\sigma}{\rho_g v_g^2}$$

and more generally, for a wave of unknown shape with $j_g \approx v_g$ we get

$$\delta_f \approx \frac{C'\sigma}{\rho_g j_g^2} \tag{12}$$

It was found that $C' = 0.375$ seems to work rather well in connection with the annulus experiments. Introducing Eq.(12) into Eq.(6) will give a result resembling a flooding correlation. Introducing $C_w = 0.005$, $C' = 0.375$ and the nondimensional fluxes we obtain:

$$1.33 = j_g^{*2} \left[1 + 8.9\times10^{-3} N_B \; j_g^{*2} + 4.0\times10^{-3} N_B^3 \; j_g^{*4} \; j_f^{*2}\right] \tag{13}$$

where

$$N_B = \frac{g D^2 (\rho_f - \rho_g)}{\sigma} \tag{14}$$

is the so called Bond number (Wallis 1969). For zero penetration, $j_f^* = 0$, we obtain for the gas flux

$$j_g^* = \left[\frac{-1 + \sqrt{1 + 4\times1.33\times8.9\times10^{-3} N_B}}{2\times8.9\times10^{-3} N_B}\right]^{1/2} \tag{15}$$

if $4\times1.33\times8.9\times10^{-3} N_B >> 1$

or

$$N_B >> 21 \tag{16}$$

The gas flux at zero penetration becomes approximately independent of the gap size and we get from eq. (15)

$$j_g^* = 3.5 \quad \frac{1}{N_B^{1/4}} \tag{17}$$

which is equivalent to a Kutateladze number

$$Ku = j_g^* N_B^{1/4} = 3.5 \tag{18}$$

which was approximately the value observed in large pipes and in the annulus.

The Bond number of a 1" annulus gap and air-water is approximately $N_B = 350$, thus eq.(16) is satisfied.

The flooding correlation of eq. (13) was used to compare with the experimental results. If only one wall is assumed to be wet the liquid flux is approximately only half the value calculated in this equation.

The agreement between the theoretical predictions and the experiments is satisfying, especially for the 1" gap (see Figures 17 and 18).

6. DISCUSSION

ZERO PENETRATION

There is some uncertainty in measuring the air velocity needed to prevent penetration of the water into large tubes as well as in annuli. In this work it was found that zero penetration in large tubes (6" or more) can be predicted with a Kutateladze number of approximately Ku = 3.2. In the annulus experiments the zero penetration in the 1" gap evaluated at approximately Ku = 3.4 and in the 2" gap at Ku = 3.0, but for the non-symmetrical top flooding experiments in the 2" gap it was closer to Ku = 3.2. Thus in general a Ku = 3.2 as predicted by Pushkina and Sorokin will predict zero penetration to about 7% accuracy for the results obtained here. It is not certain if this can be said for larger scale annuli. Rothe et.al.(1978) suggest zero penetration for a constant dimensionless J_g^* with the circumference as a characteristic length, (see Eq.(3)). This means that the gas velocity for zero penetration should increase with increase in scale. In Figure 19, J_g^* is plotted versus the scale of different annulus experiments. At small scales the constant gas flux seems to be appropriate, which is equivalent to the Wallis correlation. The experimental results presented here seem to indicate that a deviation from this line might occur at larger scale. Whether or not data from larger systems can be predicted by a Kutateladze number is too early to predict at this point. Larger scale tests should allow better conclusions to be drawn; at 1/10th scale the difference between the predictions of the J* and Ku theories is too small to be discriminated by the precision of the experiments.

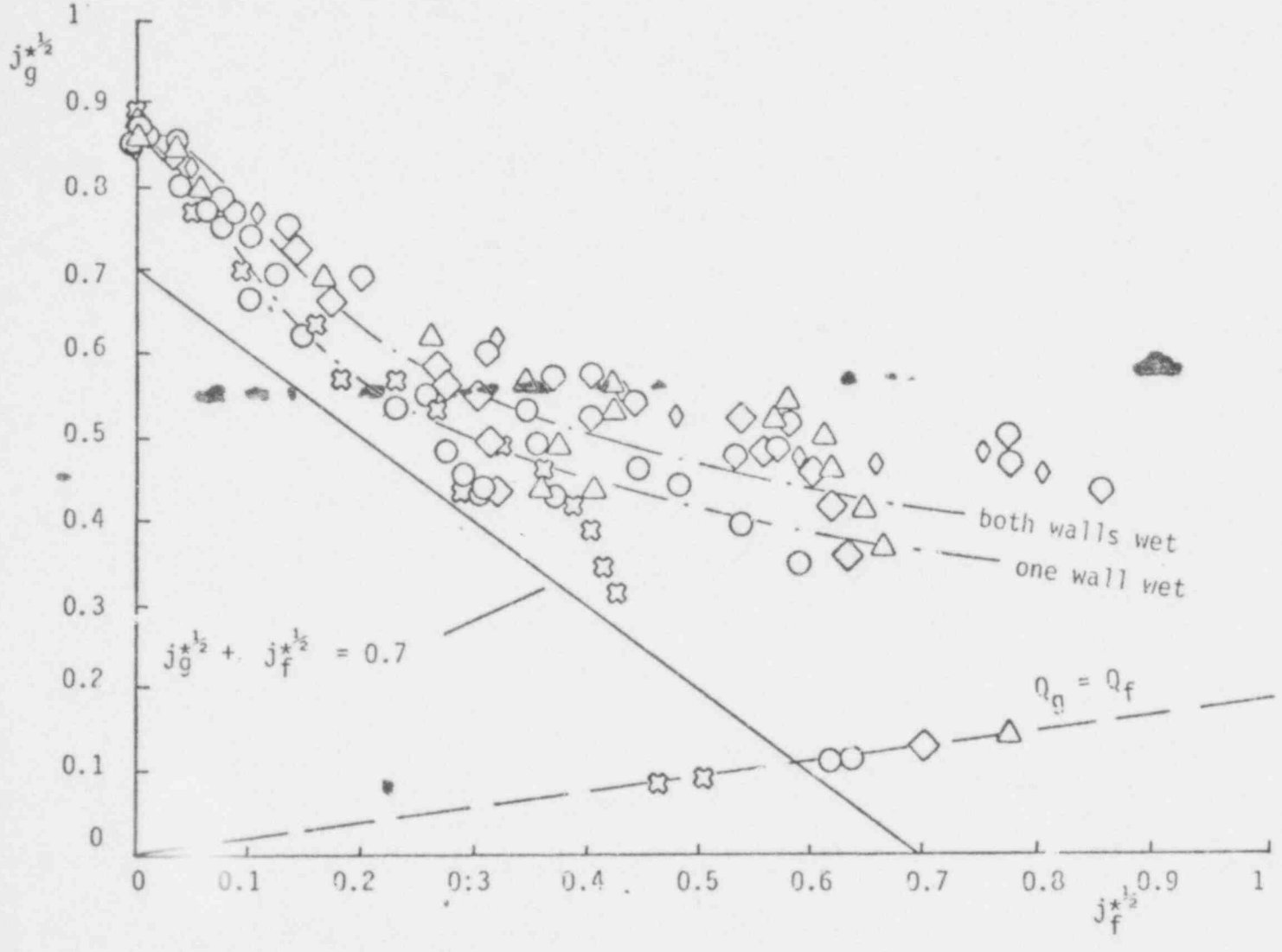

Figure 17 Nondimensional gas flux vs. water flux in the 1 inch annulus gap. Comparison with theoretical predictions.

491 117

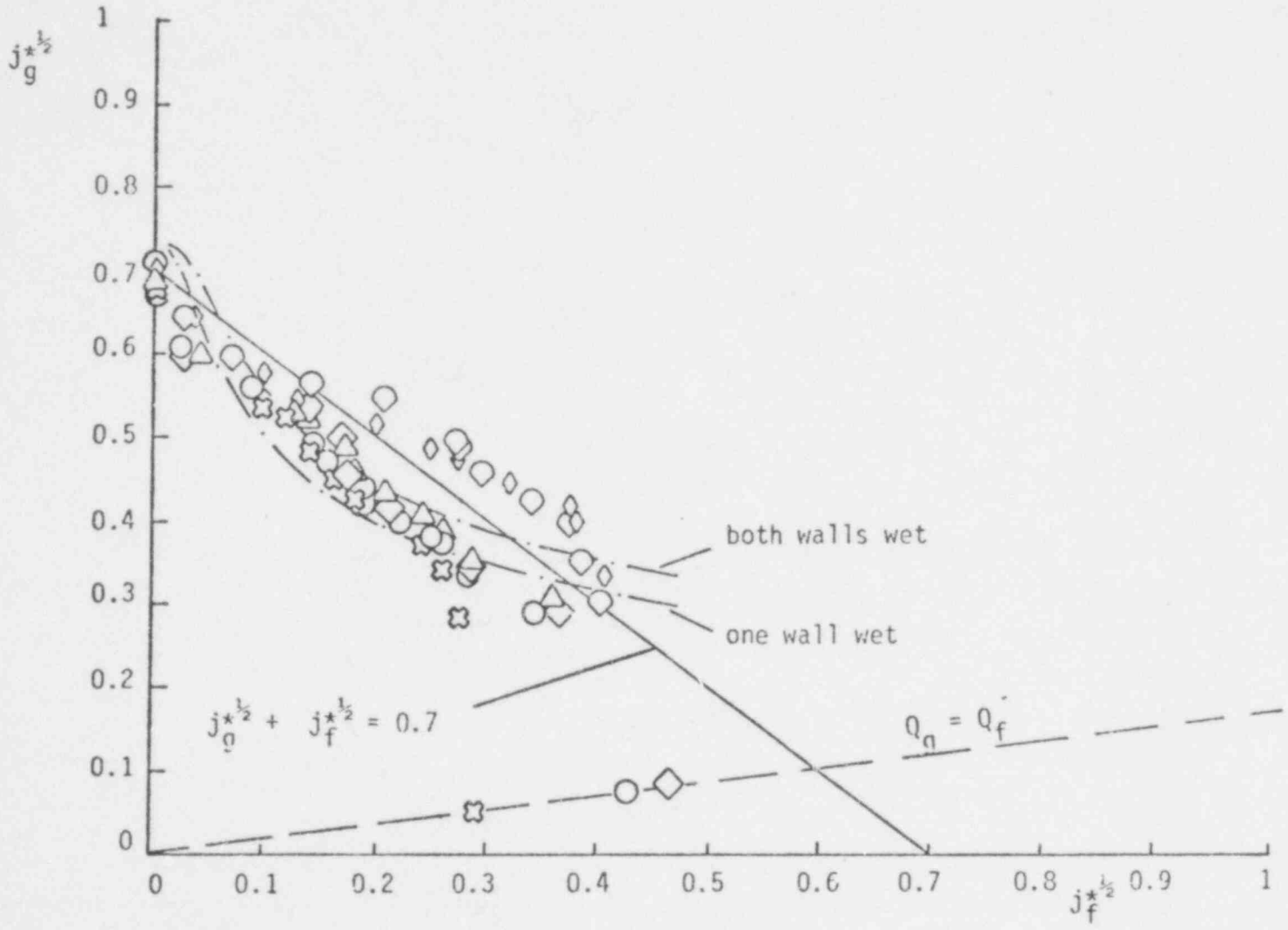

Figure 18 Nondimensional gas flux vs. water flux in the 2 inch annulus gap. Comparison with theoretical predictions.

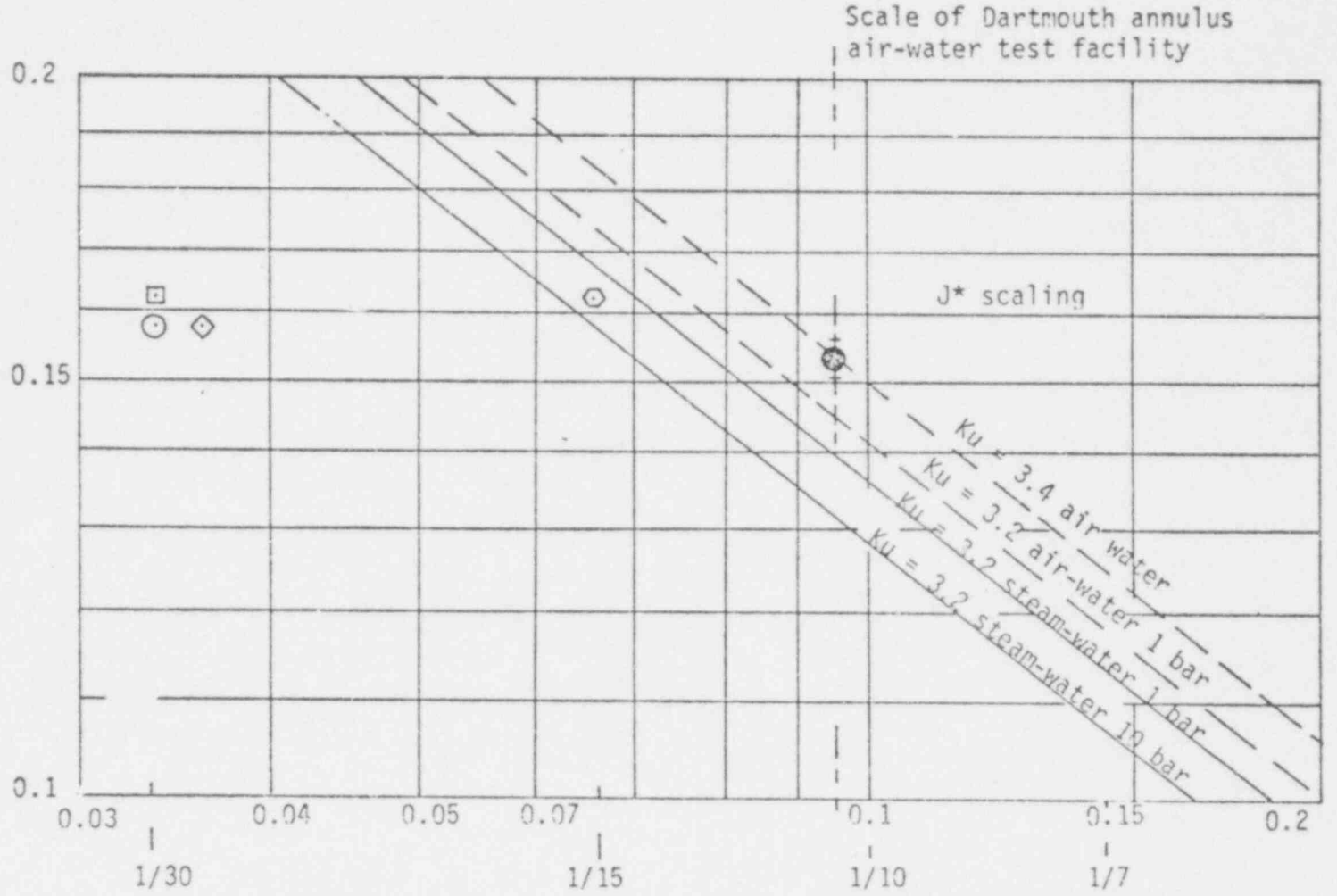

Figure 19 Nondimensional flux vs. scale of experiment.

FLOODING

While the Wallis flooding correlation was confirmed in 2" diameter tubes, it was found that in large tubes and in annuli the flooding behavior could be predicted satisfactorily with a theory derived from a simple force balance on the liquid film penetrating down the wall, assuming the film thickness was limited by surface tension (Weber number effects). The assumption of only one or both walls wetted in the annulus seems to explain the differences in flooding behavior for different water levels in the upper plenum above the top of the annulus. For low water levels obviously only one wall, in general the outside wall, seems to carry most of the liquid.

EFFECTS OF ASYMMETRY

Nonsymmetrical top flooding enhances the penetration rate only in the annulus. There it creates a highly nonsymmetrical flow pattern allowing much higher penetration rates at low gas flow rates. Close to the zero penetration point at relatively high gas flow rates the liquid entering the annulus is distributed around the annulus creating a very uniform flow pattern. Thus zero penetration occurs at approximately the same gas flux in symmetrical and nonsymmetrical top flooding.

EFFECTS OF INLET WATER MOMENTUM

It was found that water penetration could be enhanced by injecting the water from a tube or nozzle pointing downwards into the air flow. Though no quantitative understanding of this phenomenon has been reached in this study, this effect may explain some of the influence of injected flow rate on water delivery in tests using a model of a PWR annulus and injection of water through one or more of the "cold legs"

7. CONCLUSIONS

1) In both the 6" and 10" diameter tubes and the 17.5" O.D. annulus with 1" or 2" gap the zero penetration point was predicted within 7% by a Kutateladze number of 3.2.

2) The air flow at the zero penetration point for the 1/10th scale annulus lies midway between the predictions of the $J^* = 0.16$ and $Ku = 3.2$ theories and is only 7% from either of them. Larger scale tests are needed in order to obtain a less equivocal discrimination.

3) The flooding data for the 2" diameter tube correlated with the Wallis correlation. On the other hand, results from 6" and 10" tubes and from

the 17.5" O.D. annulus were represented quite closely by a theory based on a force balance for the falling film assuming a thickness determined by a Weber Number criterion.

4) Both asymmetry in the methods of introducing the water and introduction in the form of a jet can increase the rate of penetration. These effects have not been quantified in this work.

8. REFERENCES

Pushkina, O.L.; Y.L. Sorokin: Breakdown of Liquid Film Motion in Vertical Tubes. Heat Transfer Soviet Research 1(1969) 5

Richter, H.J.; T.W. Lovell: The Effect of Scale on Two-Phase Countercurrent Flow Flooding in Vertical Tubes. NRC Contract AT(49-24)-0329, August 1977

Rothe, P.H.; C.J.Crowley; J.A. Block: Progress on ECC Bypass Scaling. CREARE TN-272, NUREG/CR-0048, March 1978

Wallis, G.B.: One Dimensional Two-Phase Flow, McGraw Hill Book Company, New York 1969.

491 121

APPENDIX A. DATA OF ANNULUS EXPERIMENTS

Experiment: 1 inch annulus gap - symmetrical top flood

Water Height in Upper Plennum	Volumetric Gas Flow Rate Q_g	Volumetric Water Flow Rate Q_f	$j_g^{*\frac{1}{2}}$	$j_f^{*\frac{1}{2}}$	Δp^*
$\times 10^{-1}$ m	$\times 10^{-1}$ m^3/s	$\times 10^{-3}$ m^3/s	$\times 10^{-1}$	$\times 10^{-1}$	
0.127	1.0087	2.2472	4.3406	3.0852	0.300
0.127	2.0272	0.7874	5.7082	1.8263	0.700
0.127	3.2524	0.2144	6.9639	0.9529	1.050
0.127	4.1008	0.0670	7.6940	0.5326	1.200
0.127	5.5890	0.0000	8.8854	0.0000	1.300
0.127	1.0122	2.0115	4.3320	2.9189	0.300
0.127	0.0513	5.1282	0.8488	4.6607	0.000
0.127	2.5554	0.6079	6.3352	1.6047	1.150
0.127	1.9?22	1.2658	5.6845	2.3155	0.350
0.127	1.6517	1.6667	5 3410	2.6570	0.400
0.127	1.3186	2.5000	4.9183	3.2541	0.400
0.127	1.1030	3.1250	4.5999	3.6382	0.200
0.127	0.8599	3.5714	4.1690	3.8894	0.150
0.127	0.7249	3.8462	3.8968	4.0363	0.100
0.127	0.5346	4.0816	3.4529	4.1580	0.100
0.127	0.4203	4.3478	3.1419	4.2914	0.060
0.127	0.0505	6.0606	0.9227	5.0667	0.000
0.254	1.0389	2.2523	4.3802	3.0687	0.250
0.254	1.7115	1.2781	5.3879	2.3268	0.350
0.254	2.4710	0.5187	6.2160	1.4822	0.450
0.254	2.9333	0.2449	6 6453	1.0184	0.450
0.254	3.6614	0.2525	7.4146	1.0342	1.000
0.254	0.9858	2.2436	4.2970	3.0827	0.500
0.254	5.4360	0.0000	8.7506	0.0000	1.500
0.254	5.2468	0.0052	8.6113	0.1485	0.650
0.254	3.1458	0.3683	6.9288	1.2491	1.200
0.254	3.5480	0.2494	7.2888	1.0278	1.100
0.254	3.7458	0.1537	7.4408	0.8069	1.000
0.254	4.0637	0.0960	7.7082	0.6378	1.000
0.254	4. 505	0.0397	8.0186	0.4100	1.300
0.254	5. 4[illegible]	0.0181	8.4835	0.2767	0.800
0.254	0.925	3.3019	4.2968	3.7398	0.350
0.254	1.1165	2.0202	4.5251	2.9253	0.200
0.254	1.3211	1.8018	4.8456	2.7626	0.200
0.254	3.9590	0.1894	7.6773	0.8957	2.100
0.254	0.0972	9.7222	1.1687	6.4173	0.000
0.254	1.7742	1.5873	5.5398	2.5930	0.450
0.254	1.5643	2.8571	5.3542	3.4788	0.500
0.254	1.2879	3.0303	4.9267	3.5827	0.550
0.254	1.0336	4.7619	4.6248	4.4911	0.450

cont'd: 1 inch annulus gap - symmetrical top flood

Water Height in Upper Plenum	Volumetric Gas Flow Rate Q_g	Volumetric Water Flow Rate Q_f	$j_g^{*\frac{1}{2}}$	$j_f^{*\frac{1}{2}}$	Δp^*
x 10^{-1} m	x $10^{-1} m^3/s$	x $10^{-3} m^3/s$	x 10^{-1}	x 10^{-1}	
0.254	0.9094	5.5556	4.4206	4.8510	0.350
0.254	0.6786	6.8966	3.9684	5.4048	0.200
0.254	0.4821	8.3333	3.5021	5.9412	0.050
0.254	0.0909	9.0909	1.1301	6.2054	0.000
0.381	4.0371	0.1535	7.7163	0.8064	2.200
0.381	3.4391	0.4785	7.2467	1.4236	2.450
0.381	2.7970	0.7042	6.6275	1.7271	2.400
0.381	2.0365	1.6807	5.8556	2.6681	1.500
0.381	0.9961	2.4096	4.3280	3.1948	0.750
0.381	0.1167	11.6667	1.2802	7.0297	0.000
0.381	1.3205	2.3256	4.9211	3.1386	0.650
0.381	1.8246	1.7699	5.6207	2.7381	0.800
0.381	1.5688	4.2553	5.4864	4.2455	0.650
0.381	1.7075	2.1739	5.5028	3.0345	1.100
0.381	1.8370	1.8182	5.6465	2.7751	0.800
0.381	1.2954	6.8966	5.2152	5.4048	0.700
0.381	1.0675	7.4074	4.8129	5.6014	0.400
0.381	0.9193	8.6957	4.5910	6.0690	0.400
0.381	0.7149	9.0909	4.1601	6.2054	0.250
0.381	0.4951	9.5238	3.5800	6.3514	0.050
0.381	0.1167	11.6667	1.2802	7.0297	0.000
0.508	3.0370	0.6515	6.9138	1.6612	3.300
0.508	4.3787	0.0779	7.9894	0.5744	2.650
0.508	5.0402	0.0284	8.4976	0.3469	2.300
0.508	2.3283	1.6129	6.2250	2.6138	3.150
0.508	3.9570	0.1505	7.6477	0.7983	2.500
0.508	5.5687	0.0000	8.8621	0.0000	2.000
0.508	5.4886	0.0000	8.7981	0.0000	2.000
0.508	0.9924	3.0702	4.3907	3.6062	0.850
0.508	1.2528	3.3333	4.9078	3.7576	1.000
0.508	0.9413	3.9216	4.3658	4.0756	0.900
0.508	0.1429	14.2857	1.4167	7.7789	0.000
0.508	1.7804	2.8571	5.6876	3.4788	1.000
0.508	1.5025	4.2553	5.3867	4.2455	0.900
0.508	1.2854	7.6923	5.2516	5.7081	0.600
0.508	1.3977	8.0000	5.4556	5.8212	0.700
0.508	1.6671	4.2553	5.6528	4.2455	0.600
0.508	1.1346	8.8889	5.0343	6.1361	0.450
0.508	0.9316	9.0909	4.6402	6.2054	0.350
0.508	0.6888	10.0000	4.1240	6.5083	0.270

cont'd: 1 inch annulus gap - symmetrical top flood

Water Height in Upper Plenum	Volumetric Gas Flow Rate Q_g	Volumetric Water Flow Rate Q_f	$j_g^{*\frac{1}{2}}$	$j_f^{*\frac{1}{2}}$	Δp^*
$\times 10^{-1}$ m	$\times 10^{-1}$ m^3/s	$\times 10^{-3}$ m^3/s	$\times 10^{-1}$	$\times 10^{-1}$	
0.508	0.5244	10.5263	3.6976	6.6774	0.300
0.508	0.1167	11.6667	1.2802	7.0297	0.000
1.016	2.0689	2.2989	6.0292	3.1205	3.400
1.016	2.9809	0.9434	6.9202	1.9590	4.250
1.016	3.6946	0.4274	7.5172	1.3454	4.000
1.016	4.1880	0.1377	7.8704	0.7638	4.000
1.016	4.7819	0.0402	8.3096	0.4127	3.500
1.016	1.7719	3.2258	5.7248	3.6965	3.600
1.016	1.4204	3.8462	5.2245	4.0363	2.200
1.016	1.0579	6.7308	4.7734	5.3395	2.000
1.016	5.0696	0.0347	8.5514	0.3835	3.500
1.016	5.5513	0.0000	8.8556	0.0000	3.400
1.016	1.0671	7.6923	4.8357	5.7081	1.900
1.016	1.7525	3.8462	5.7330	4.0363	1.400
1.016	1.5172	4.6512	5.4310	4.4386	1.300
1.016	1.2291	8.0000	5.1690	5.8212	1.200
1.016	1.0229	14.2857	5.0120	7.7789	1.000
1.016	0.8541	14.2857	4.6550	7.7789	0.400
1.016	0.6901	17.3913	4.3284	8.5829	0.400
1.524	5.1334	0.0000	8.4611	0.0000	4.400
1.524	0.9894	8.3333	4.7241	5.9412	3.200
1.524	4.6310	0.0673	8.2175	0.5341	4.500
1.524	3.937	0.2759	7.7008	1.0810	4.700
1.524	2.135	2.4096	6.1142	3.1948	5.350
1.524	0.9269	10.2941	4.6739	6.6033	2.300
1.524	1.6246	4.4444	5.5927	4.3389	2.300
1.524	1.3717	5.4795	5.2597	4.8176	2.100
1.524	0.9416	13.4615	4.8320	7.5512	1.650
1.524	0.8046	15.3846	4.5707	8.0725	1.700

Experiment: 1 inch annulus gap - nonsymmetrical top flood

Water Height in Upper Plenum	Volumetric Gas Flow Rate	Volumetric Water Flow Rate	$j_g^{*\frac{1}{2}}$	$j_f^{*\frac{1}{2}}$	Δp^*
x 10^{-1} m	x 10^{-1} m^3/s	x 10^{-3} m^3/s	x 10^{-1}	x 10^{-1}	
0.254	1.0822	3.2787	4.5322	3.7266	0.080
0.254	1.6704	3.2787	5.5316	3.7266	0.200
0.254	2.5388	1.2270	6.4494	2.2798	2.250
0.254	3.7199	0.1739	7.4370	0.8583	1.750
0.254	3.6316	0.1734	7.3485	0.8571	1.650
0.254	4.4119	0.0678	7.9910	0.5359	1.500
0.254	5.5964	0.0000	8.8609	0.0000	1.400
0.254	0.0370	3.7037	0.7213	3.9608	0.000
0.254	1.7066	3.5651	5.6427	3.8860	0.150
0.254	1.4871	3.5088	5.2812	3.8552	0.100
0.254	1.0195	3.5273	4.5052	3.8 54	0.050
0.254	0.8318	3.5088	4.1093	3.8552	0.050
0.254	0.5697	3.5398	3.4955	3.8722	0.000
0.254	1.9321	3.4783	5.9338	3.8384	0.150
0.254	0.0374	3.7383	0.7247	3.9793	0.000
1.016	1.0037	7.2917	4.7180	5.5575	1.250
1.016	2.1225	4.0816	6.2662	4.1580	4.150
1.016	3.6286	1.1905	7.5994	2.2456	4.200
1.016	0.1129	11.2903	1.2594	6.9154	0.000
1.016	4.1979	0.5420	8.0110	1.5152	3.000
1.016	4.6763	0.2825	8.3361	1.0939	2.700
1.016	5.7132	0.0000	8.9923	0.0000	2.000
1.016	1.7355	7.7519	5.9723	5.7302	1.500
1.016	1.9139	6.2696	6.1606	5.1533	5.150
1.016	1.5014	8.5106	5.6552	6.0041	1.000
1.016	1.0924	10.2041	5.018	6.5744	0.750
1.016	0.8242	10.4790	4.4680	6.6623	0.500
1.016	0.6048	10.5422	3.9418	6.6824	0.350
1.016	0.1087	10.8696	1.2357	6.7854	0.000

*

Experiment: 2 inch annulus gap - symmetrical top flood

Water Height in Upper Plenum	Volumetric Gas Flow Rate Q_g	Volumetric Water Flow Rate Q_f	$j_g^{*\frac{1}{2}}$	$j_f^{*\frac{1}{2}}$	Δp^*
$\times 10^{-1}$ m	$\times 10^{-1}$ m^3/s	$\times 10^{-3}$ m^3/s	$\times 10^{-1}$	$\times 10^{-1}$	
0.127	0.0532	5.3191	0.5303	2.9120	0.000
0.127	4.1120	1.2308	4.9490	1.4007	0.250
0.127	4.7707	0.8889	5.2444	1.1904	0.350
0.127	5.4753	0.5392	5.5588	0.9270	0.450
0.127	6.8850	0.0694	6.0891	0.3327	0.430
0.127	8.6347	0.0000	6.7702	0.0000	0.020
0.127	4.9979	0.5993	5.3463	0.9779	0.500
0.127	3.3791	1.7391	4.5341	1.6651	0.200
0.127	4.0503	1.2270	4.8908	1.3986	0.250
0.127	3.7195	1.5267	4.7200	1.5601	0.250
0.127	2.9738	2.1053	4.3017	1.8320	0.180
0.127	2.5575	2.8986	4.0679	2.1496	0.150
0.127	2.0936	3.7453	3.7657	2.4435	0.150
0.127	1.6924	4.2105	3.4517	2.5908	0.100
0.127	1.0555	4.7619	2.8407	2.7552	0.100
0.254	0.1143	11.4286	0.7773	4.2684	0.000
0.254	4.1580	1.3072	4.9678	1.4436	0.400
0.254	4.7004	1.0929	5.2364	1.3200	0.500
0.254	5.5579	0.4988	5.5965	0.8917	0.700
0.254	6.8753	0.0392	6.0731	0.2499	0.500
0.254	8.6536	0.0000	6.7690	0.0000	0.020
0.254	3.6984	1.5504	4.7135	1.5721	0.400
0.254	3.2376	1.9512	4.4672	1.7637	0.400
0.254	2.8809	2.4845	4.2682	1.9902	0.400
0.254	2.4635	3.1250	4.0163	2.2320	0.250
0.254	2.0768	4.2105	3.7818	2.5908	0.250
0.254	1.6894	5.0633	3.4903	2.8411	0.200
0.254	1.0491	7.4906	2.9283	3.4556	0.150
0.381	0.1364	13.6364	0.8491	4.6625	0.000
0.381	4.0457	1.7467	4.9446	1.6687	0.500
0.381	4.6960	1.2539	5.2521	1.4139	0.700
0.381	6.7052	0.0422	6.0095	0.2592	0.700
0.381	8.6472	0.0000	6.7629	0.0000	0.050
0.381	1.0469	8.3333	2.9543	3.6448	0.250
0.381	1.5523	5.1948	3.3771	2.8778	0.250
0.381	2.1790	3.8095	3.8479	2.4644	0.370
0.381	2.6687	2.7586	4.1449	2.0971	0.550
0.381	3.1385	2.3256	4.4344	1.9255	0.450
0.381	3.4782	1.8519	4.6135	1.7182	0.430
0.508	3.9746	1.8433	4.9176	1.7142	0.600

cont'd: 2 inch annulus gap - symmetrical top flood

Water Height in Upper Plenum	Volumetric Gas Flow Rate Q_g	Volumetric Water Flow Rate Q_f	$j_g^{*\frac{1}{2}}$	$j_f^{*\frac{1}{2}}$	Δp^*
$\times 10^{-1}$ m	$\times 10^{-1}$ m^3/s	$\times 10^{-3}$ m^3/s	$\times 10^{-1}$	$\times 10^{-1}$	
0.508	4.8860	1.0336	5.3365	1.2836	0.900
0.508	4.6859	1.2422	5.2524	1.4073	0.850
0.508	6.6017	0.1101	6.0166	0.4190	0.900
0.508	9.0893	0.0000	6.9427	0.0000	0.020
0.508	3.8891	1.8921	4.8640	1.7368	0.620
0.508	3.4102	2.0408	4.5807	1.8037	0.500
0.508	2.9371	2.7027	4.3257	2.0757	0.500
0.508	2.5421	3.6697	4.1069	2.4187	0.550
0.508	2.1497	4.2105	3.8381	2.5908	0.450
0.508	1.6907	5.1282	3.4995	2.8593	0.350
0.508	1.1270	8.1633	3.0370	3.6075	0.250
1.016	3.7303	4.5977	4.9438	2.7073	1.250
1.016	5.4321	1.2500	5.6402	1.4116	1.670
1.016	4.8036	2.6144	5.4232	2.0415	1.620
1.016	6.3664	0.3086	5.9376	0.7015	1.580
1.016	7.6638	0.0447	6.4468	0.2670	0.600
1.016	9.1104	0.0000	6.9570	0.0000	0.250
1.016	1.0914	10.2564	3.0619	4.0436	0.900
1.016	1.5802	9.3023	3.5547	3.8509	0.400
1.016	2.1209	8.6957	4.0016	3.7232	0.950
1.016	2.5103	7.1429	4.2483	3.3745	0.950
1.016	3.1063	5.4054	4.5921	2.9355	1.050
1.016	3.4201	4.6512	4.7549	2.7230	1.120
1.524	3.6138	3.8835	4.8510	2.4882	1.500
1.524	5.0200	1.1527	5.4500	1.3556	2.000
1.524	4.3467	2.4845	5.1817	1.9902	2.000
1.524	5.9233	0.6061	5.7922	0.9829	2.250
1.524	7.6512	0.0785	6.4599	0.3537	1.400
1.524	9.0413	0.0000	6.9438	0.0000	0.080
1.524	3.2792	4.7619	4.6788	2.7552	1.750
1.524	2.8810	6.4516	4.4881	3.2070	1.750
1.524	2.4267	8.8889	4.2497	3.7644	1.750
1.524	2.1123	9.0909	4.0106	3.8069	1.250
1.524	1.3754	10.3627	3.3777	4.0645	1.350

*

Experiment: 2 inch annulus gap - nonsymmetrical top flood

Water Height in Upper Plenum	Volumetric Gas Flow Rate, Q_g	Volumetric Water Flow Rate, Q_f	$j_g^{*\frac{1}{2}}$	$j_f^{*\frac{1}{2}}$	Δp^*
$\times 10^{-1}$ m	$\times 10^{-1}$ m^3/s	$\times 10^{-3}$ m^3/s	$\times 10^{-1}$	$\times 10^{-1}$	
0.254	2.2914	3.4483	3.9293	2.3446	0.020
0.254	1.8044	3.4483	3.5216	2.3446	0.020
0.254	0.6143	3.4783	2.2018	2.3548	0.010
0.254	4.6547	3.4247	5.3831	2.3366	0.600
0.254	5.2217	1.1111	5.5086	1.3309	0.900
0.254	5.3339	1.0363	5.5610	1.2853	0.850
0.254	5.5830	0.7194	5.6491	1.0709	0.800
0.254	0.0339	3.3898	0.4234	2.3247	0.000
0.254	6.5277	0.1304	5.9546	0.4560	0.750
0.254	6.2508	0.2433	5.8623	0.6228	0.700
0.254	5.5353	0.4854	5.7677	0.8797	0.700
0.254	5.7135	0.6579	5.6870	1.0241	0.700
0.254	5.1065	1.2121	5.4578	1.3901	0.800
0.254	4.9792	1.4493	5.4141	1.5200	0.800
0.254	4.6652	3.1746	5.3721	2.2496	0.800
0.254	4.1394	3.4783	5.0937	2.3548	0.200
0.254	3.5850	3.3898	4.7608	2.3247	0.120
0.254	2.6379	3.3898	4.1367	2.3247	0.050
0.254	8.6332	0.0000	6.7410	0.0000	0.100
1.016	0.1575	15.7480	0.9125	5.0105	0.000
1.016	2.3848	15.6250	4.3878	4.9909	0.200
1.016	6.3309	3.3333	6.2329	2.3052	2.000
1.016	6.0306	4.0404	6.1321	2.5379	1.850
1.016	5.5587	5.1471	5.9650	2.8645	1.750
1.016	4.9571	6.1162	5.6986	3.1226	1.700
1.016	4.2300	7.2202	5.3483	3.3927	1.700
1.016	3.0357	10.9589	4.7316	4.1798	1.600
1.016	2.5915	13.7931	4.4957	4.6892	1.450
1.016	8.1770	0.7220	6.7977	1.0729	2.120
1.016	9.7963	0.0000	7.2149	0.0000	1.250
1.016	7.2517	1.8957	6.5293	1.7384	1.900
1.016	7.7379	1.2963	6.6730	1.4375	1.250
1.016	7.0365	2.3256	6.4553	1.9255	1.200
1.016	5.8325	4.7619	6.0438	2.7552	1.150

*

APPENDIX B. CALCULATION OF LIQUID VOLUME FLOW RATE FOR NONSYMMETRICAL TOP FLOOD (FLOW OVER A WEIR)

In the diagram (see Figure 7) with the experimental results for nonsymmetrical top flood theoretical points are also plotted, where the liquid volume flow rate is equal to the gas volume flow rate ($Q_g = Q_f$). These points were obtained by calculation of the flow over a weir, which is

$$Q_f = \frac{2}{3} \mu b \, h \sqrt{2 \, g \, h} \tag{A1}$$

where μ is a weir coefficient, usually $\mu = 0.63$, b is the width of the weir, in this case one quarter (90^o) of the circumference as long as the water height is less than 3 inches and h is the water height above the weir. For the nondimensional flux we receive then for the water flow down if $\rho_f >> \rho_g$

$$j_f^* = \frac{8\sqrt{2}}{3\pi} \mu \frac{b \, h^{3/2}}{D^{5/2}} \quad , \tag{A2}$$

with D the diameter of the pipe and since $Q_g = Q_f$

$$j_g^* = \left(\frac{\rho_g}{\rho_f}\right)^{1/2} j_f^* \tag{A3}$$

UNITED STATES
NUCLEAR REGULATORY COMMISSION
WASHINGTON, D. C. 20555

OFFICIAL BUSINESS
PENALTY FOR PRIVATE USE, $300

POSTAGE AND FEES PAID
U.S. NUCLEAR REGULATORY
COMMISSION

S Scott LA212

120555031837 2 ANR2
US NRC
SECY PUBLIC DOCUMENT ROOM
BRANCH CHIEF
HST LOBBY
WASHINGTON DC 20555

491 131